

K. DORUK

FIBER REINFORCED POLYMER CONFINED  
RC CIRCULAR COLUMNS SUBJECTED TO  
AXIAL LOAD AND BENDING MOMENT

KORAY DORUK

JULY 2006

METU  
2006

FIBER REINFORCED POLYMER CONFINED  
RC CIRCULAR COLUMNS SUBJECTED TO  
AXIAL LOAD AND BENDING MOMENT

A THESIS SUBMITTED TO  
THE GRADUATE SCHOOL OF NATURAL AND APPLIED SCIENCES  
OF  
MIDDLE EAST TECHNICAL UNIVERSITY

BY

KORAY DORUK

IN PARTIAL FULFILLMENT OF THE REQUIREMENTS  
FOR  
THE DEGREE OF MASTER OF SCIENCE  
IN  
CIVIL ENGINEERING

JULY 2006

Approval of the Graduate School of Natural and Applied Sciences

---

Prof. Dr. Canan ÖZGEN  
Director

I certify that this thesis satisfies all the requirements as a thesis for the degree of Master of Science

---

Prof. Dr. Erdal ÇOKCA  
Head of Department

This is to certify that we have read this thesis and that in our opinion it is fully adequate, in scope and quality, as a thesis for the degree of Master of Science

---

Associate Prof. Dr. Barış BİNİCİ  
Supervisor

**Examining Committee Members**

Prof. Dr. Güney ÖZCEBE	(METU)	_____
Assoc. Prof. Dr. Barış BİNİCİ	(METU)	_____
Asst. Prof. Dr. Erdem CANBAY	(METU)	_____
Assoc. Prof. Dr. Ahmet Yakut	(METU)	_____
Dr. Bekir Afşin CANBOLAT	(YÜKSEL PROJE)	_____

**I hereby declare that all information in this document has been obtained and presented in accordance with academic rules and ethical conduct. I also declare that, as required by these rules and conduct, I have fully cited and referenced all material and results that are not original to this work.**

Name, Last Name: Koray DORUK

Signature :

## **ABSTRACT**

### **FIBER REINFORCED POLYMER CONFINED RC CIRCULAR COLUMNS SUBJECTED TO AXIAL LOAD AND BENDING MOMENT**

Doruk, Koray

M.Sc., Department of Civil Engineering

Supervisor: Assoc. Prof. Dr. Barış Binici

July 2006, 79 pages

Fiber reinforced polymers (FRPs) have gained increasing popularity in upgrades of reinforced structural elements due to high strength to weight ratio and ease of application. In this study, the effectiveness of the carbon reinforced polymer wrapping (CFRP) on ductility and strength of circular reinforced concrete columns, made of low strength concrete, is presented. Four circular reinforced columns with similar dimensions, longitudinal and confining steel reinforcement were tested under combined axial load and bending moment. Three specimens were strengthened with CFRP and the results were compared with the control specimen. The main parameter of the experimental study was selected as the level of eccentricity. First of all, the strain profiles of FRPs in the circumferential direction were observed and the confining stress distributions were examined. Then, an axial stress-strain model for FRP confined concrete with a transition from softening to hardening response for different confinement ratios is proposed. The proposed model was verified by comparing the model estimations with the test results obtained from this study and results reported by other researches. In addition, a parametric study was presented to obtain a simple equation to estimate curvature ductility of FRP confined circular columns.

Keywords: Fiber Reinforced Polymers (FRPs), confinement, ductility, design

## ÖZ

### EKSENEL YÜK VE EĞİLME MOMENTİ ALTINDAKİ LİFLİ POLİMER SARGILI DAİRESEL BETON KOLONLAR

Doruk, Koray

Yüksek Lisans, İnşaat Mühendisliği Bölümü

Tez Yöneticisi: Doç. Dr. Barış Binici

Temmuz 2006, 79 sayfa

Lifli polimerler, yüksek dayanım-ağırlık oranı ve kolay uygulanabilme özelliklerine sahip olduklarından dolayı betonarme yapı elemanlarının güçlendirilmesinde tercih edilir hale gelmiştir. Bu çalışmada, karbon lifli polimerlerle sarılmış kolonların sünekliği ve dayanımı incelenmiştir. Dört adet aynı boyut ile aynı boyuna ve sargı donatısına sahip olan dairesel betonarme kolon, bileşik eksenel yük ve eğilme altında test edilmiştir. Bu kolonlardan üç tanesi karbon lifli polimer ile güçlendirilmiş ve test sonuçları güçlendirilmemiş kolondan elde edilen test sonuçlarıyla karşılaştırılmıştır. Deneysel çalışmadaki ana parametre ise dışmerkezliktir. Ayrıca lifli polimerin sargı yönündeki deformasyon profilleri ve sargı gerilme dağılımı elde edilmiştir. İkinci olarak, lifli polimer sargılı kolonların yumuşamadan sertleşmeye kadar davranışlarının geniş bir sargı aralığını kapsayan eksenel gerilme-deformasyon davranışı, bir modelle ortaya konulmuştur. Deneysel çalışma ve diğer araştırmacıların yapmış olduğu çalışmalar, ortaya konulan bu modelin kullanılmasıyla yeniden analiz edilip, elde edilen sonuçlar deneylerle karşılaştırılmış ve modelin doğruluğu gösterilmiştir. Ayrıca modelin doğruluğu sağlandıktan sonra, lifli polimer sargılı dairesel kolonların süneklik katsayısını veren bir denklem elde etmek parametrik bir çalışma da son kısımda yapılmıştır.

Anahtar Kelimeler: Lifli Polimerler, sargı, süneklik, tasarım

## ACKNOWLEDGEMENTS

I would like to express my sincere thanks and appreciation to Assoc. Prof. Dr. Barış Binici who not only encouraged me for this study but also supported me about my private problems. His suggestions and guidance encouraged me to complete this study. It was a great honor and pleasure to work with him.

I also would like to convey my endless appreciation to my parents and sister for their confidence in me. They tried to make all conditions good for me to complete this study.

I also should thank my friends and other members of the faculty for their friendship and support.

This study was conducted under the financial support from BAP 2003-03-03-05.

## TABLE OF CONTENTS

<b>PLAGIARISM.....</b>	<b>III</b>
<b>ABSTRACT .....</b>	<b>IV</b>
<b>ÖZ.....</b>	<b>V</b>
<b>ACKNOWLEDGEMENTS.....</b>	<b>VI</b>
<b>TABLE OF CONTENTS.....</b>	<b>VII</b>
<b>LIST OF TABLES .....</b>	<b>IX</b>
<b>LIST OF FIGURES .....</b>	<b>X</b>
<b>CHAPTER</b>	
<b>1. INTRODUCTION.....</b>	<b>1</b>
1.1. LITERATURE SURVEY.....	4
1.1.1. Studies on FRP Confined Concrete.....	4
1.1.2. Studies on FRP Wrapped Columns under Combined Axial Load and Bending Moment .....	9
1.2. OBJECTIVES AND SCOPE.....	12
<b>2. EXPERIMENTAL PROGRAM.....</b>	<b>14</b>
2.1. GENERAL.....	14
2.2. TEST SPECIMENS.....	14
2.3. MATERIAL PROPERTIES .....	17
2.4. TEST SETUP AND INSTRUMENTATION .....	18
2.5. TEST RESULTS.....	19
<b>3. MODELING AND PARAMETRIC STUDIES.....</b>	<b>25</b>
3.1. FRP CONFINED CONCRETE MODEL DESCRIPTION.....	25
3.2. VERIFICATION OF THE MODEL .....	32
3.2.1. Verification of the Model with Experimental Results from This Study .....	33
3.2.2. Verification of the Model with the Paper of Sheikh and Yau [13].....	37
3.3. PARAMETRIC STUDIES .....	42

<b>4. CONCLUSION.....</b>	<b>51</b>
<b>REFERENCES .....</b>	<b>54</b>
<b>APPENDICES .....</b>	<b>57</b>
<b>A. TABLE OF THE PARAMETRIC STUDY .....</b>	<b>59</b>

## LIST OF TABLES

### TABLE

2.1	Properties of Test Specimens .....	17
3.1	Properties of the Columns in the Paper of Sheikh and Yau [13] .....	37
3.2	Properties of the FRP Composites in the Paper of Sheikh and Yau [13].....	38
3.3	Properties of the Reinforcement Steel in the Paper of Sheikh and Yau [13] .....	38
3.4	Material Properties of the Reinforcement Steel .....	43
3.5	Material Properties of the CFRP .....	43
3.6	Details of Analysis .....	44
3.7	List of the Slopes and Initial Constants of Equation of the Linear Fits on the Graphs of Figure 3.9 .....	49
A.1	The Values of the Parameters of the Each Column and Results of the Parametric Study .....	59

## LIST OF FIGURES

### FIGURE

2.1	Cross-Section Details of the Specimens.....	15
2.2	Test Specimen and Setup .....	16
2.3	Moment-Curvature and Axial Load Curvature Results .....	21
2.4	Test Specimens after Failure .....	22
2.5	Axial and Lateral Response of Specimen 4 .....	22
2.6	Interaction Diagrams .....	23
2.7	Confining Stress Distribution For Specimen 4 .....	24
3.1	FRP Confined Concrete Model.....	28
3.2	Comparison of the Stress Enhancement Factor of Softening and Hardening Behavior of the FRP Confined Concrete .....	29
3.3	Comparison of the Moment-Curvature Relationship of Specimen 1 with respect to Experimental and Analytical Study .....	34
3.4	Comparison of the Moment-Curvature Relationship of Specimen 2 with respect to Experimental and Analytical Study .....	35
3.5	Comparison of the Moment-Curvature Relationship of Specimen 3 with respect to Experimental and Analytical Study .....	35
3.6	Comparison of the Moment-Curvature Relationship of Specimen 4 with respect to Experimental and Analytical Study .....	36
3.7	Comparison of the Moment-Curvature Relationships of the Unconfined Specimens with respect to Paper [13] and Analytical Study.....	39
3.8	Comparison of the Moment-Curvature Relationships of the FRP Confined Specimens with respect to Paper [13] and Analytical Study.....	340
3.9	Relationship between Ductility Factor and Confinement Ratio with respect to the Axial Load Ratio and Longitudinal Reinforcement Ratio .....	45

3.10	Ductility Factor-Longitudinal Reinforcement and Axial Load Ratio For $\Phi=0.40$ and $D=2000$ mm .....	47
3.11	Comparison of the Ductility Factors from Equation 3.20 and Sectional Analysis Comparisons of Model with Data in Literature .....	50

## **CHAPTER 1**

### **INTRODUCTION**

A structure should be designed and constructed to be economical and in compliance with the code specified design criteria. The main objective of the structural engineers is to find the optimum solution to the engineering problem such that construction of the structure is feasible and safety of it is not compromised. In most of the current building codes, structures are designed so that strength is not exceeded due to the combined action of vertical and horizontal loads. Furthermore, for seismic resistance, energy dissipation capacity is provided to the structure through necessary detailing of critical regions. The input energy on the structure is usually dissipated by yielding, cracking, plastic hinging etc. of the structural members which appear as visual damage. An implied performance criteria in the form of “allow damage and avoid collapse” is aimed to be satisfied by controlling certain damage indicators such as storey deformations.

After the 1999 earthquakes in Turkey, many structures collapsed or sustained high damage. The fact that the building stock is highly vulnerable has come to the attention of the engineering community, although it was known well before these catastrophic events. Most of the vulnerable structures in Turkey have not been designed for prescribed earthquake forces or they lack the necessary detailing. This necessitates establishment of reliable strengthening methodologies so that the expected loss in future earthquakes is minimized. With this objective, a new section on seismic evaluation and rehabilitation has been added to the recent draft version of the Turkish Earthquake Resistant Design Code. In this way, it was aimed to unify the evaluation and rehabilitation procedures and guide the engineers in determining vulnerable members or parts of a structural system. In this new document, a section was also added on the use of fiber reinforced

polymers to enhance deformation capacity of columns subjected to combined action of axial force and bending moment.

Fiber reinforced polymers (FRPs) have gained increasing popularity in upgrade projects for strengthening of reinforced structural elements. High modulus fibers embedded in a resin matrix are used to bind the fibers to form FRPs. There are three common fiber types: carbon, glass and aramid. These FRP types are called carbon fiber reinforced polymers (CFRP), glass fiber reinforced polymers (GFRP) and aramid-fiber reinforced polymers (AFRP). All these types of FRPs have a linear elastic stress-strain behavior and exhibit a brittle failure upon reaching their strain limit. Their advantages such as being lightweight, high strength, non-corrosive, and ease of application have made them an excellent choice of material for structural retrofits. FRPs have found a wide variety of applications such as use in deteriorating bridges, strengthening of deficient beams for flexure and shear, and columns for shear, axial load and deformation capacity enhancement. Although FRPs exhibit a brittle behavior compared to steel, due to their high strain limits, when used as confining material, they can increase the ductility of concrete members.

Ductility can be defined as the ability of sustaining large inelastic deformations without any significant change in the load carrying capacity of a member or structure. As the available ductility increases, the likelihood of the structure against collapse can decrease in the case displacement controlled loading, for example during seismic action. Confinement is provided to restrain deformations and minimize unstable dilatation due to cracking. Test results revealed that behavior of FRP-confined concrete substantially differs from that of steel confined concrete due to differences in constitutive behavior of the two materials. For steel confined concrete, confining stresses are proportional to the applied axial load up to the yielding of the steel. Beyond yielding of the transverse steel reinforcement, confining stresses remain approximately constant. On the other hand, for FRP confined concrete, the level of confinement increases with imposed axial strains up to the point where FRP ruptures and failure occurs in a sudden and brittle manner. Therefore, confinement mechanisms are different for

steel and FRP confined concrete, therefore it is not possible to use available steel confined concrete models in FRP design.

Insufficient lateral stiffness due to gravity load design and improper detailing of columns, beams and beam – column joints, insufficient lap splice and anchorage length are some of the reasons of the observed earthquake damage in the buildings in Turkey. When these reasons of damages are examined, it can be seen that additional ductility and strength should be added to reduce seismic risk. The two strengthening methods, namely addition of a new lateral force resisting system or member strengthening can be employed for this purpose. These two methods are different views of attacking the same problem and most probably, the optimum solution is the use of both approaches together. Hence guidelines to employ either of them should be at service of structural engineers.

One of the most important applications in member strengthening is the strengthening of reinforced concrete columns to enhance their axial load and deformation capacities. Both steel and FRP jacketing is possible in this regard. Due to its advantages outlined above, use of FRPs has gained popularity in reinforced concrete column retrofits. Wrapping, filament winding, and use of prefabricated shell jacketing are the three ways of strengthening of columns by FRPs. The most common way of strengthening of columns is wrapping in which the FRP sheets are wrapped around columns. This method has the advantage of application flexibility for different column shapes. On the other hand, it has disadvantages due to difficulty of quality control. In FRP wrapping technology, the columns are wrapped completely with one or more layers of FRPs after impregnating them with the epoxy resin. In filament winding process, FRP is wrapped using strands in a similar way to FRP wrapping, the only difference being the method of wrapping. It provides better quality control opportunity than wrapping, but it exhibits less flexibility for different column shapes. In the prefabricated shell jacketing method, half circle or half rectangle FRP shells are fabricated under close inspection using either fiber sheets or strands. If the contact of the FRP and the column is carefully established, significant confinement

enhancement can be possible. This method shows the best quality control but its flexibility for different column shapes is limited.

The shape of the columns is also an important factor on the effectiveness of the FRP confinement. Wrapping of circular columns is more effective than wrapping of rectangular columns. Therefore, a shape modification (i.e. changing the section from rectangular to an elliptical section) can be needed before applying the FRPs. In addition, types of the fibers and resin, bond between column face and jacket, concrete strength, jacket thickness, length / diameter ratio of the column are the other parameters that can influence the effectiveness of the FRP confinement and long term performance.

## **1.1 LITERATURE SURVEY**

Studies conducted in the literature reveal that confinement provided by FRP wrapping can improve both axial load carrying capacity and the ductility of the column. In this section, first, some of the important experimental and analytical studies on axially loaded FRP confined concrete are briefly reviewed. Then, studies conducted on strengthening of columns subjected to lateral reversed-cyclic loading are presented.

### **1.1.1 Studies on FRP Confined Concrete**

There is a vast amount of experimental and analytical research on axial response of FRP confined concrete. Only a number of important studies are reviewed below.

Mirmiran et. al. [1] studied the effect of the column parameters on FRP confined concrete. Shape, bond and size effect of columns were investigated in their study. Twelve 152.5 x 152.5 x 305 mm square cylinders and thirty 152.5 x 305 mm cylindrical specimens were constructed and tested under axial compression. It was observed that square columns exhibited lower strength at FRP rupture than their peak strength whereas for circular specimens ultimate strength was substantially higher than uniaxial compressive strength. It was seen that the

thickness of the jacket affected the confinement performance of the circular sections more than square sections. Similar to steel-confined concrete both cross-sections had a volume reduction under axial load up to a limit but after this point the volume expanded. This behavior was independent from the shape of cross-section but dependent on the thickness of the jacket. A modified confinement ratio (MCR) was defined and beyond a critical value of MCR, no softening was observed. In the second part of the study twenty-four FRP confined concrete cylindrical specimens were constructed to examine the length effect. The main parameters were the thickness of jacket and the length of the specimens. The length to diameter ratios (L/D) of the specimens was in the range of 2:1 to 5:1. As a result of the experiment it was seen that there were not any significant effect of specimen length on the behavior of the FRP confined concrete. According to the test results the maximum accidental eccentricity was seen as the 10 - 12 % of the section width. Authors concluded that standard 2:1 aspect ratio cylinders were acceptable to examine the effect of aspect ratio. Final parameter studied in the experimental program was the bond between FRP and concrete. Two different bonding techniques were applied with different number of layers. One of them was adhesive bonding; epoxy was used for bonding the concrete core and FRP jacket and the other type was mechanical bond in which mechanical shear connectors were used as bonding material. According to the test results the authors mentioned that the adhesive bond did not affect the load carrying capacity but mechanical bond improved the confinement pressure significantly.

Tan et. al. [2] examined the effect of fiber type, configuration and fiber anchors of the FRP on the strength improvement of the rectangular reinforced columns. In addition, an analytical approach was presented to calculate the axial load capacity of the FRP confined columns using the model proposed by Wang and Restrepo [3]. The rectangular columns had a maximum aspect ratio of 3.65:1. 52 short columns were constructed and ten of them were tested as control specimens with no FRPs. The parameters were number of plies of fiber sheets, presence of plaster finishes, and number of rows of the fiber anchor bolts, bonding of the fiber sheets and type of the fiber sheets. It was observed that transverse

fiber sheets confined specimens, decreased the lateral dilatation and increased the axial load capacity of the column. The higher axial load capacities were obtained by anchoring transverse fiber sheets along the wider faces of the column. Delamination along the length of the column was seen on the GFRP wrapped specimens more than those with CFRP sheets.

Xiao and Wu [4] presented the stress-strain results of the CFRP confined concrete cylinders under axial compression and developed a simple stress-strain model using those test results. 36 concrete cylinders were constructed and 27 of those were confined with CFRP jackets. The main parameters of the specimens were the thickness of the CFRP jackets and compressive strength of the cylinders. The failure of the confined concrete occurred at the onset of rupture of the CFRP jacket but the rupture strain obtained from the tension test of the CFRP sheets was much higher than the observed average rupture strain of the jacket (about 1.5 times). It was observed that the CFRP jacket increased significantly strength and ductility of concrete. With increasing jacket stiffness, higher strength and ductility was noted. The authors mentioned that confinement strength and the confinement modulus affected the performance of the specimens. Using theory of elasticity for axially loaded axisymmetric problems and test results, equations relating transverse strains to axial strains and a bilinear axial stress-strain model were proposed.

Ilki and Kumbasar [5] investigated the effect of the CFRP wrapping on axially loaded circular, square and rectangular (1:2 aspect ratio) concrete specimens having low to normal strength concrete (10 to 30MPa). In their study, undamaged and pre-damaged specimens were tested under monotonic and repeated compressive loads. Failure of all specimens was due to sudden and brittle FRP rupture. As the thickness of the CFRP jacket was increased, higher strength and deformation capacity was observed. The relative strength increase of low-strength concrete was more pronounced compared to that observed in normal strength concrete. However, ultimate axial strain at FRP rupture was barely affected from concrete uniaxial compressive strength. It was also observed that the axial stress- axial strain behavior of the monotonic loading curve was the envelope curve of the cyclic loading cases. The pre-damaged and strengthened

specimens showed similar behavior compared to strengthened specimens without any prior damage. Therefore, it was stated that the pre-damaging did not have an adverse effect on the behavior of the CFRP confined concrete. The CFRP confined square concrete specimen with one layer showed an increase in deformability but the strength enhancement was limited. With increasing jacket stiffness, higher ductility and ultimate strength was achieved for specimens with circular and square sections. For square and rectangular sections, it was found that the efficiency of the confining mechanism can be improved by rounding off the corners of the sections. Finally, a simple analytical model was proposed and verified to estimate the ultimate strength and ultimate axial strain of CFRP confined concrete with square, rectangular and circular cross sections in the study.

Many stress-strain models for FRP confined concrete have been proposed in the past and these models can be classified into two groups. First group is design-oriented models. These models define an axial stress-strain relationship for FRP confined concrete as a function of compressive strength and ultimate axial strain, which are determined from empirical equations calibrated with test results. The second group is the analysis-oriented models in which the behavior of the FRP confined concrete is determined through incremental analysis by satisfying lateral compatibility. In these models, interaction between concrete and jacket is directly taken into account.

Spoelstra and Monti [6] presented an axial stress-strain model for concrete confined with FRP or steel jackets. This model clearly demonstrated the continuous interaction between the confining jacket and core using an incremental-iterative approach. The starting point of the model was the stress strain model of the Mander et. al. [7] which was based on the stress-strain equations of Popovics et. al. [8] for concrete under constant active confinement. In employing the model, for a given axial strain, the axial stress was computed from the corresponding confined concrete curve for the lateral pressure applied by the jacket that satisfied lateral deformation equivalency between the jacket and concrete. A lateral expansion damage model proposed by the Pantazopoulou and Millis [9] was used in order to calculate lateral strain at a given level of axial

strain. When the model estimations of axial stress-strain response were compared with the tests of wrapped cylinders, a reasonable agreement was observed. The authors also mentioned that this model was more effective in moment curvature analyses than the commonly used confinement models at the cost of more calculations.

Binici [10] developed a confined concrete model to determine axial and lateral deformation characteristics of concrete under tri-axial compression. The verification and the parametric studies were also presented. In the model, the stress- strain relationship of the confined concrete started with an elastic region and continued with a nonlinear curve. A constant energy failure was used for determining the descending part of the stress- curve of the confined concrete. Leon-Pramono criterion was used to determine the ultimate strength, elastic limit, and residual strength of confined concrete. Lateral deformations were obtained using secant strain ratios. The model was compared with the experimental results and it was observed that the use of the model resulted in sufficiently accurate estimations of confined concrete behavior for axisymmetric problems. Later this model was extended to combined axial and bending situations and was implemented in a fiber-frame finite element program [11]. In their implementation, a bond stress model was used to estimate the confining stress distribution in the compression zone.

Lam and Teng [12] proposed a design-oriented stress-strain model for FRP confined concrete using a database of 76 axial compression tests. Following four assumptions were employed for the model: 1) Stress-strain curve of the FRP confined concrete has a parabolic first region and a straight line second portion. 2) Initial slope of the confined concrete curve is not affected by the amount of confinement (i.e. modulus of elasticity of FRP confined concrete is same as that in the case of unconfined concrete). 3) There is a smooth transition from nonlinear region to the hardening linear part of the curve. 4) The compressive strength and the ultimate axial strain occurs at the same point which is the end of the second portion. According to these assumptions the proposed stress-strain curve was given as a function of compressive strength of concrete, ultimate effective strain

of FRP. The authors concluded that in their stress-strain model, effective FRP strain should be the actual rupture strain measured in the axial tests rather than the ultimate material tensile strength reported by the manufacturer. Based on a review of the test database it was concluded that effective rupture strain was about 60% of the ultimate tensile strain reported by the manufacturer for CFRPs. The proposed model was flexible to be used for concrete confined with different types of FRPs. The advantage of the model was its simplicity for use in sectional analysis. However, the model is not realistic for situations when the FRP confined concrete response exhibits a descending softening branch. This phenomenon can be encountered for circular columns with small number of FRP layers or for bridge columns with large section diameter and for rectangular columns with a smaller degree of confinement efficiency.

### **1.1.2 Studies on FRP Wrapped Columns under Combined Axial Load and Bending Moment**

Sheikh and Yau [13] studied the effect of CFRP and GFRP wrapping on the strengthening of circular columns. 12 test specimens were prepared for this study and these specimens were divided into three groups: reference specimens, strengthened specimens with no prior damage, and strengthened damaged specimens. Each column had a 356 mm diameter with a length of 1470 mm and a column stub of 510 x 760 x 810 mm. The first group included four specimens with deficient and code compliant spiral reinforcement designs with two axial load levels of 0.54 and 0.27. These four columns had two different volumetric ratios of the transverse steel, (1.12% and 0.30%). The six test specimens, which were in the second group, had volumetric lateral reinforcement ratio of 0.30 with similar concrete strength of the specimens as in group one (40 MPa). The only difference was strengthening of the columns in-group two by CFRPs and GFRP with different number of layers. The last group consisted of two specimens that had a volumetric lateral reinforcement ratio of 0.56% and specimens in this group were first damaged by imposing lateral deformation under constant axial load and then repaired using GFRP and CFRP after removal of all the loads. The main objective of this study was to observe the effect of the FRPs on the columns'

behavior under earthquake forces, hence the specimens were tested under constant axial load and reversed cyclic load. It was reported that energy dissipation of the strengthened columns increased about 100 times resulting in a superior ductility compared to the un-strengthened ones. It was observed that FRP wrapped specimens exhibited a response as good as, if not better, than those with code compliant designs. The effect of prior damage on the column tended to decrease the deformability of the sections; however no qualitative conclusions were deduced.

Iacobucci et. al. [14] investigated the effectiveness of the CFRP strengthening on the behavior of square reinforced concrete columns under simulated earthquake forces. Eight column specimens were constructed in dimensions of 305 x 305 x 1473 mm with a 508 x 762 x 813 mm stub. The specimens consisted of three groups which were control specimens, retrofitted specimens and damaged retrofitted specimens. All these specimens had similar volumetric ratio of the rectilinear ties of 0.61% with normal strength concrete (~40 MPa). The specimens were designed according to the construction practice of 1970s, i.e. these columns did not have sufficient transverse reinforcement according to the current code requirements. The control group had three specimens which had no strengthening and were loaded with axial load ratios ( $P/P_o$ ) of 0.33, 0.33 and 0.56. The retrofitted group had five specimens; two of them with one layer of the CFRP and were loaded with axial load ratios of 0.33 and 0.56; the other two had 2 layer of CFRP and were loaded with axial load ratios of 0.33 and 0.56; the last specimen of the retrofitted group had 3 layer CFRP and was loaded with an axial load ratio of 0.56. Cyclic lateral displacement excursions were applied to the specimens while maintaining the axial load constant to simulate seismic loading. It was reported that the CFRP jackets increased reinforced columns' ductility, energy dissipation, and moment capacities. It was observed that high axial load levels decreased the effective performance of the CFRP jackets so the authors mentioned that the number of FRP layers should be increased at high axial load level to have same performance at low axial load levels. It was seen that FRP jacket improved the performance of

the deficient columns to a level as good as the ones with sufficient lateral reinforcement in relevant code provisions. No recommendations regarding jacket design was proposed.

Harajli and Rteil [15] examined the effect of CFRP jacket on the seismic behavior of reinforced concrete columns that was designed only for gravity loads with lap splices at the column base. The CFRP was wrapped in the critical hinging zone of the columns. In addition, two reinforced concrete columns with well-detailed stirrups were constructed to compare the effects of FRP confinement and steel confinement at critical regions. The parameters in the test program were the amount of longitudinal reinforcement in the columns, volumetric ratio of steel fibers and area of the steel fibers. There were two groups of specimens in the study. In the first group, the specimens had a longitudinal reinforcement ratio of 1.5% and five of these specimens had a volumetric lateral reinforcement ratio of 0.445% and the last specimen in the first group had lateral reinforcement ratio of 0.89%. The second group had a longitudinal reinforcement ratio of 2.7% and the value of the lateral reinforcement ratios of this group were the same as the first group. In each group there were six specimens and two of these specimens were wrapped with CFRP and the other two of the specimens were confined with steel fibers with volumetric steel ratios of 1% and 2%, respectively. In each group, one of the columns had a CFRP jacket of 300 mm wide layer and the other column had a 300 mm wide layer with three 50 mm wide strips. Specimens in first and second group were loaded under constant axial compression force of 22 and 26 tons, respectively, and lateral loading cycles under a displacement control mode. The columns, which were designed for gravity loads without any external confinement showed serious bond deterioration under cyclic loading. On the other hand, it was observed that wrapping the critical zone of the column with CFRP increased both bond strength and deformation capacity of the column and decreased the bond deterioration. Steel confinement also improved the seismic behavior since the bond deterioration was delayed. CFRP confinement improved the seismic behavior of the column more effectively compared to the ordinary

transverse steel for the same area of confining reinforcement. No explicit design recommendations were proposed in their study.

Seible et. al. [16] described the CFRP jacket design criteria for reinforced concrete bridge columns considering different types of failure modes, namely, shear failure, flexure failure and lap-splice failure. It was proposed that for lap-splice strengthening, lateral dilatation of concrete in the tension region had to be limited to a strain level of about 0.0001 and corresponding lateral pressure was needed to suppress bond deterioration. Furthermore, the effective strain of FRPs in shear was proposed to be 0.004 based on the review of experimental results. For flexural strengthening the curvature ductility was computed based on a lateral pressure calculated using an effective jacket strain of 0.004. Three experiments were also conducted to verify the ability of the proposed design procedure to estimate deformation capacities. Two rectangular columns and a circular column were designed and then wrapped by CFRP whose thicknesses at each critical region of the columns were determined according to the proposed models. As a result of the tests the authors mentioned that increasing the modulus of the jacket in the hoop direction decreased the required thickness of the CFRP jacket for shear and lap-splice wrapping. On the other hand it was also mentioned that although the jacket modulus was lower, the plastic hinge confinement could be very effective to improve the ductility. Finally, authors mentioned that the differences and uncertainties in the materials and lay-up systems, curing and durability conditions should be taken into account for actual retrofit applications.

## **1.2 OBJECTIVES AND SCOPE**

In the literature examined, all the test data for concrete columns subjected to combined axial loads and bending moments was bound to compressive concrete strength values higher than about 20MPa. In addition, it was found that there is no information regarding confining stress distribution for the loading cases of combined axial and bending moment. Furthermore, none of the proposed stress-strain models can represent the FRP confined concrete behavior with a

transition from a softening to hardening response. In order to fill this gap observed in the literature, following objectives for the present study are set forth:

- 1) to examine the effect of the FRP wrapping on the ductility and strength of the low-strength circular reinforced columns which are designed for gravity loads only,
- 2) to measure and report strain profiles of FRPs in the circumferential direction and observe the confining stress distributions,
- 3) to propose a simple model for the behavior of the FRP confined concrete and to verify this model by comparing model estimations with the test results obtained from this study and results reported by other researches,
- 4) to propose a simple design equation of curvature ductility for the FRP confined circular columns as a result of the parametric study.

In this study, firstly an experimental program was conducted on circular reinforced concrete columns. Specimens were tested under combined axial load and bending moment in a monotonic manner. The parameters in the study were the presence of FRP jacket and the level of the eccentricity (i.e. ratio of bending moment to axial force).

In Chapter 2, experimental program details and test results are explained. In Chapter 3, a new FRP confined concrete model is explained and its verification with test results is presented along with the results of a parametric study. Summary and main conclusions from the study are given in Chapter 4.

## **CHAPTER 2**

### **EXPERIMENTAL PROGRAM**

#### **2.1 GENERAL**

In the experimental part of this study, four reinforced columns with similar dimensions, longitudinal and confining steel reinforcements were tested under combined axial loads and bending moments. It was aimed to examine the effect of carbon fiber reinforced polymer (CFRP) wrapping on ductility of circular reinforced columns with low compressive strength and insufficient confining steel that are commonly observed in deficient buildings in Turkey. Furthermore, the experimental results were aimed to serve as means of developing and verifying an analytical model. Three of the tested columns were strengthened by CFRPs and the results were compared with the test results of the specimen without any strengthening. The main parameter considered in this study was the level of eccentricity and the other parameter was the presence of the CFRP jacket.

#### **2.2 TEST SPECIMENS**

All specimens had similar dimensions and reinforcing steel details as shown in Figure 2.1. The height of the specimens was 1000 mm with a 200 mm diameter in the test region defined as the middle 400 mm of the test specimens which are given in Figure 2.2. It should be noted that a similar experimental test-set up was previously used successfully by Baran [23] and Dinçer [24]. The two 200 mm long heads of the specimens were designed specifically to transfer the eccentric load to the column without creating significant damage outside the test region. The lengths of 100 mm between the heads and the test region were named as the transition regions. Triangular and flat surfaces were formed on the two sides of the both heads to mount eccentric loading setup on the specimens. Three

bolt holes were left on both of the heads by using steel pipes through which 24 mm steel bolts were passed.

Each specimen had six 10 mm diameter (6Ø10) longitudinal deformed bars, which were continuous along the specimen and were uniformly distributed around the perimeter of the cage of the specimen with a clear cover of 6 mm. The cross section of the specimens is shown in the Figure 2.1. U shaped 8 mm diameter deformed bars were also used as additional confinement at the heads to carry the eccentric load. In the test region of the specimens, 4 mm diameter plain bars were used for spirals with a spacing of 120 mm. In the transition and end zones 6 mm diameter bars with 30 mm spacing were used. In this way, it was possible to ensure that the test region was critical and failure occurred in this region due to lack of confining steel or FRP rupture. Details of the reinforcement and the geometry of the specimens are shown in Figure 2.2.

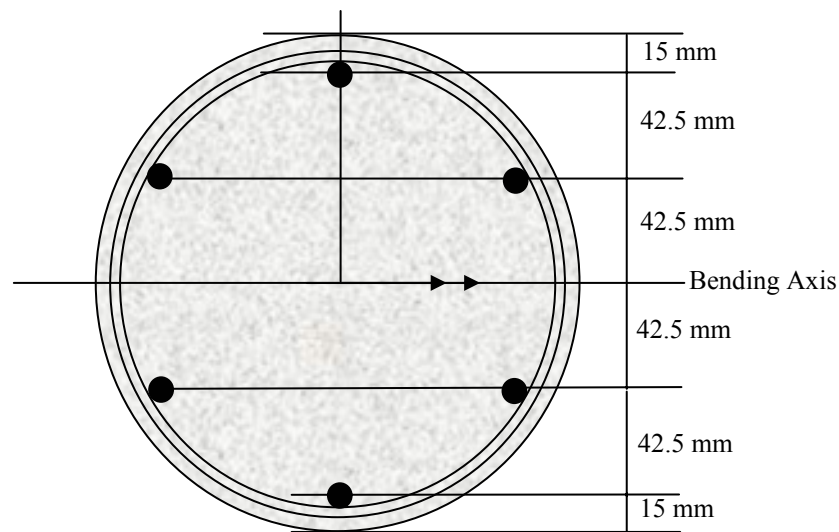


**Figure 2.1** Cross-Sectional Detail of the Specimens

Four specimens were tested in the experimental program. Specimen 1 had no FRP strengthening and served as the control specimen. Specimens 2, 3, and 4 were strengthened with 1 layer CFRPs. Prior to application of CFRPs, column surfaces cleaned from dust by air blowing. Then CFRPs impregnated into epoxy

were wrapped around the columns. During the impregnation CFRP surfaces were carefully cleaned to be dust-free. No air bubbles were left during wrapping of the CFRP jacket on the specimens. The fibers of the CFRP were oriented along the circumference direction of the columns to achieve effective confinement.

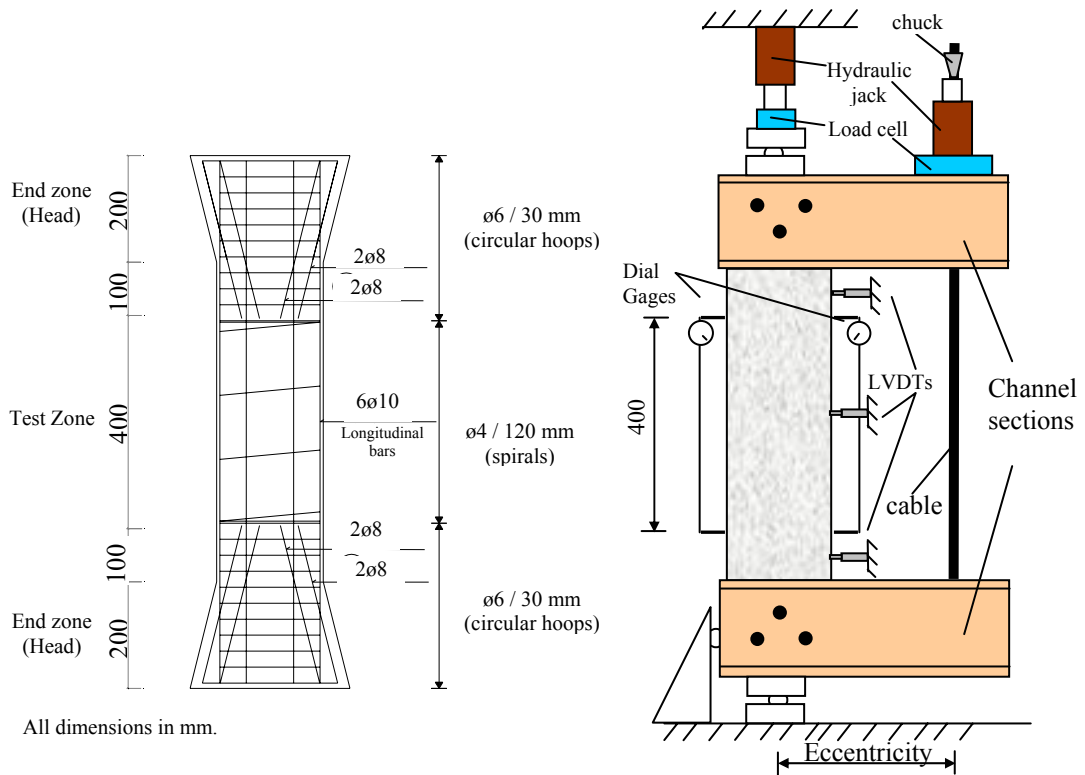


**Figure 2.2** Test Specimen and Setup

100 mm overlap of CFRP wraps were provided in order to provide sufficient anchorage. Additional CFRP patches were placed in the transition regions and heads of the specimens so that premature failure of the transition region was eliminated. After CFRP wrapping, specimens were left five days prior to testing for proper curing of epoxy resin. The properties of the test specimens are given in Table 2.1.

## 2.3 MATERIAL PROPERTIES

A target compressive strength of 10 MPa was aimed for all the specimens. Actual test day uniaxial compressive strength of the test Specimens 1, 2, 3, and 4 were 8.7 MPa, 8.9 MPa, 8.9 MPa and 9.4 MPa respectively (Table 2.1). Yield strength and ultimate strength of longitudinal bars were found as 390 MPa, and 540 MPa, respectively. On the other hand, 4 mm diameter reinforcing steel used for the spirals in the test region had yield strength of 260 MPa and an ultimate strength of 390 MPa.

**Table 2.1** Properties of the Test Specimens

<b>Properties/ Specimen No</b>	<b>1</b>	<b>2</b>	<b>3</b>	<b>4</b>
Diameter of column(mm)	200	200	200	200
Diameter of core (mm)	184	184	184	184
Diameter of Longitudinal Steel (mm)	10	10	10	10
Diameter of Lateral Steel	4	4	4	4
Spacing (mm)	120	120	120	120
$f'_c$ (MPa)	8.66	8.87	8.91	9.38
$f_y$ (MPa)	397.6	397.6	397.6	397.6
$f_{yw}$ (MPa)	261.5	261.5	261.5	261.5
Eccentricity (e) (mm)	Variable*	290	175	0
No of FRP layers	-	1	1	1

\* : Constant axial load (45% of axial load carrying capacity)

Carbon fiber reinforced polymers were used as the strengthening material for all the retrofitted specimens. Ultimate strength and modulus of elasticity of CFRPs as reported by the manufacturer was 3450 MPa and 230000 MPa, respectively, for a fiber thickness of 0.165 mm prior to impregnation with epoxy. Flat coupon tests were conducted on CFRP composites to verify manufacturer reported material properties [17]. It was found that CFRP composite after impregnation with epoxy had a thickness of approximately 1 mm with an ultimate strength and modulus of elasticity of 540 MPa and 61000 MPa, respectively.

## **2.4 TEST SETUP AND INSTRUMENTATION**

The details of test-setup are shown in Figure 2.2. A steel reaction frame was used to test all the specimens. Roller supports were placed at the ends of the specimen to prevent moment restraints at the ends. The load cell and the hydraulic jack were placed to act on the roller supports. 300 kN and 1000 kN load cells were used to measure axial loads of Specimens 1 and 4, respectively. Two U200 sections were fixed to both ends of specimens with bolts passing through 24 mm holes left using steel pipes. A steel plate was placed on the top of channel sections to locate the load cell and the hydraulic jack for eccentric loading. A 200kN load cell was used for specimens tested with constant eccentricity, namely Specimens 2 and 3. A steel tendon was passed through load cell, hydraulic jack and between the channel sections and it was fixed with chucks at the top and bottom the channel sections (Figure 2.2). The eccentric load was applied to the channels by stressing the cable with the hydraulic jack. By adjusting the location of the steel plates on the flanges, it was possible to impose different eccentricities for the test specimens.

Both hydraulic jacks were used in the testing of Specimen 1. The load applied by the hydraulic jack located in the column longitudinal axis was adjusted such that approximately constant axial load was maintained throughout the test. The axial load was kept constant between about 121 kN and 125 kN. The ratio of the applied axial load to the axial load carrying capacity for Specimen 1 was about 45%. Specimens 2 and 3 were tested with constant eccentricities of about 290 mm

and 175 mm, respectively; in the absence of any additional axial force (i.e. only one hydraulic jack was used). Specimen 4 was tested under concentric compression in order to obtain the compressive stress-strain response of FRP confined reinforced concrete as a basis of comparison.

LVDTs were used to measure the shortening and elongation of concrete at the extreme compression and tension fibers (Figure 2.2). Using these displacement measurements within the gauge length of 400 mm, curvatures (for Specimens 1, 2, and 3) and average axial strains (for Specimen 4) were computed. Furthermore, strain gauges located in the radial direction were used to determine the confining stress distribution and rupture strains for Specimen 3 and 4. For Specimen 4, additional strain gauges in the axial direction were used to verify the average strain measurements obtained from dial gauges.

## **2.5 TEST RESULTS**

The measured moment-curvature results for Specimens 1, 2 and 3 are given in Figure 2.3. Axial load-curvature relations are also presented in the same figure, since tests were performed under variable axial load in general. Pictures of specimens after testing are presented in Figure 2.4.

Specimen 1 failed in a brittle manner as a result of cover spalling followed by rebar buckling at a curvature of about 175 rad/km due to insufficient lateral restraint provided by the spirals. Specimens 2 and 3 experienced very large curvatures (above 1000 rad/km) prior to failure. Flexural cracks spaced at about 100 mm opened widely followed by an explosive popping sound. All FRP strengthened columns failed as a result of CFRP rupture in a sudden and brittle manner (Figure 2.4). It can be observed that FRP wrapping increased the ductility of the Specimens 2 and 3 significantly and they had large deformation and energy dissipation capacity. Specimen 1 had a curvature ductility of about 2, whereas specimens experienced curvature ductilities of about 15 and 12, respectively.

The axial and lateral response of Specimen 4, which was tested under concentric compression loading, along with the distribution of strain gauges is

presented in Figure 2.5. The strain gauges were located in the longitudinal and circumferential directions in the quarter perimeter of the column. Axial strains obtained from the average of dial gauge readings and strain gauge readings are both presented. It can be observed that load-strain response obtained from strain gauges and dial gauges slightly deviate from each other due to local nature of strain gauge readings. It can be stated that the axial response of FRP confined reinforced concrete column exhibited almost a bilinear response terminating at an axial strain of about 0.015. Similar to Specimens 2 and 3, failure occurred as a result of FRP rupture in a sudden and brittle manner for Specimen 4 (Figure 2.4). Transverse strains obtained from three strain gauges attached in the lateral direction show that FRP rupture occurred at a maximum FRP strain of about 0.0085, which is substantially smaller than the manufacturer's reported ultimate strain value of 0.015. This difference can be attributed to the possible accidental eccentricities and local cracking of concrete beneath FRPs that can result in premature rupture of FRP sheets.

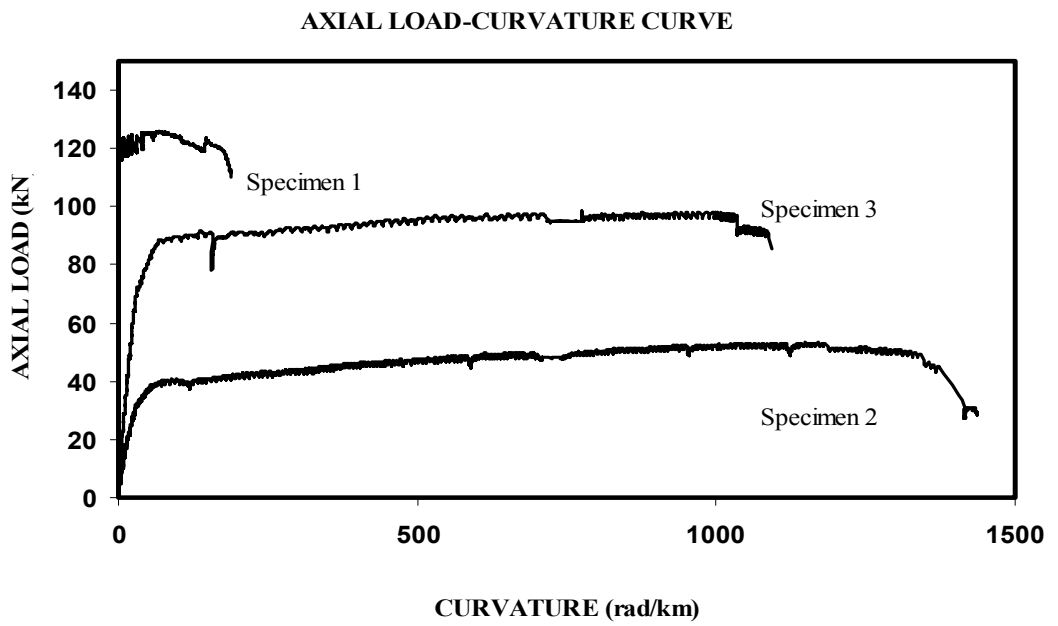
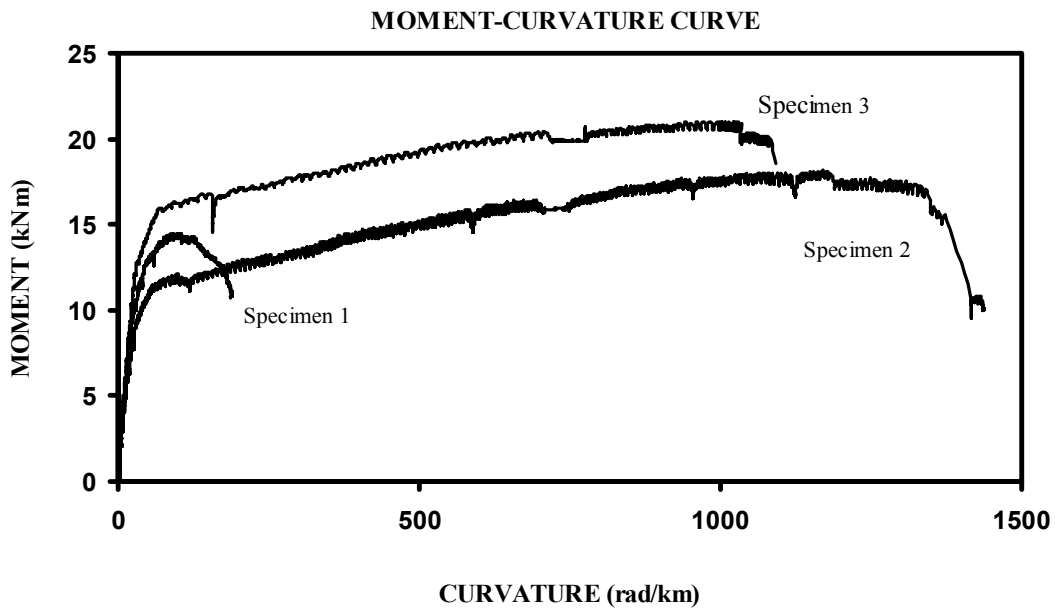


**Figure 2.3** Moment-Curvature and Axial Load-Curvature Results

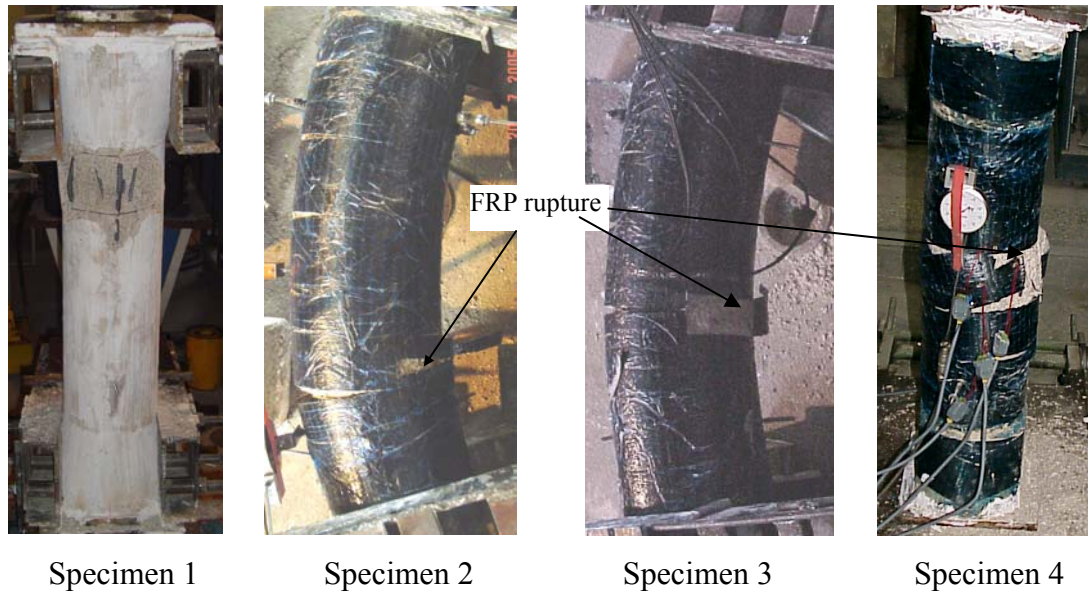


**Figure 2.4** Test Specimens after Failure

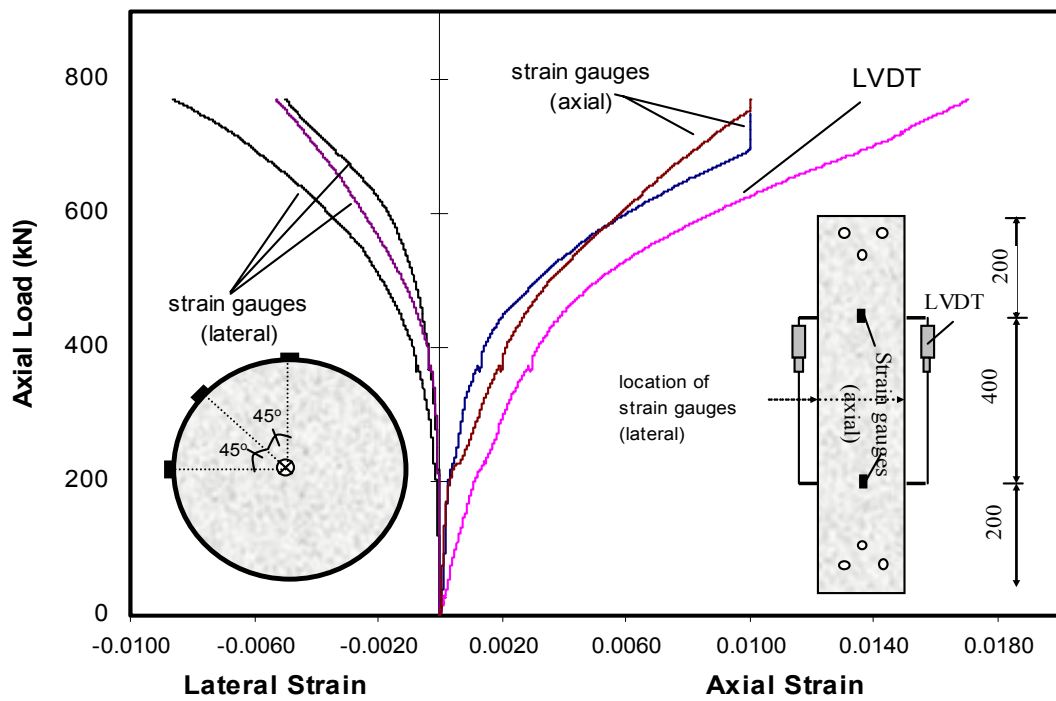


**Figure 2.5** Axial and Lateral Response of Specimen 4

Axial load bending moment interaction diagrams was obtained using the test results presented above. The interaction diagram for the specimen without any strengthening (Specimen 1) was obtained numerically using a sectional analysis program. It can be observed that FRP wrapping resulted in both moment and axial load capacity increases. Especially for lower eccentricities, the axial load capacity increases significantly for specimens made of low strength concrete. FRP wrapping was also found to significantly influence the location of the balanced point as can be observed in Figure 2.6.

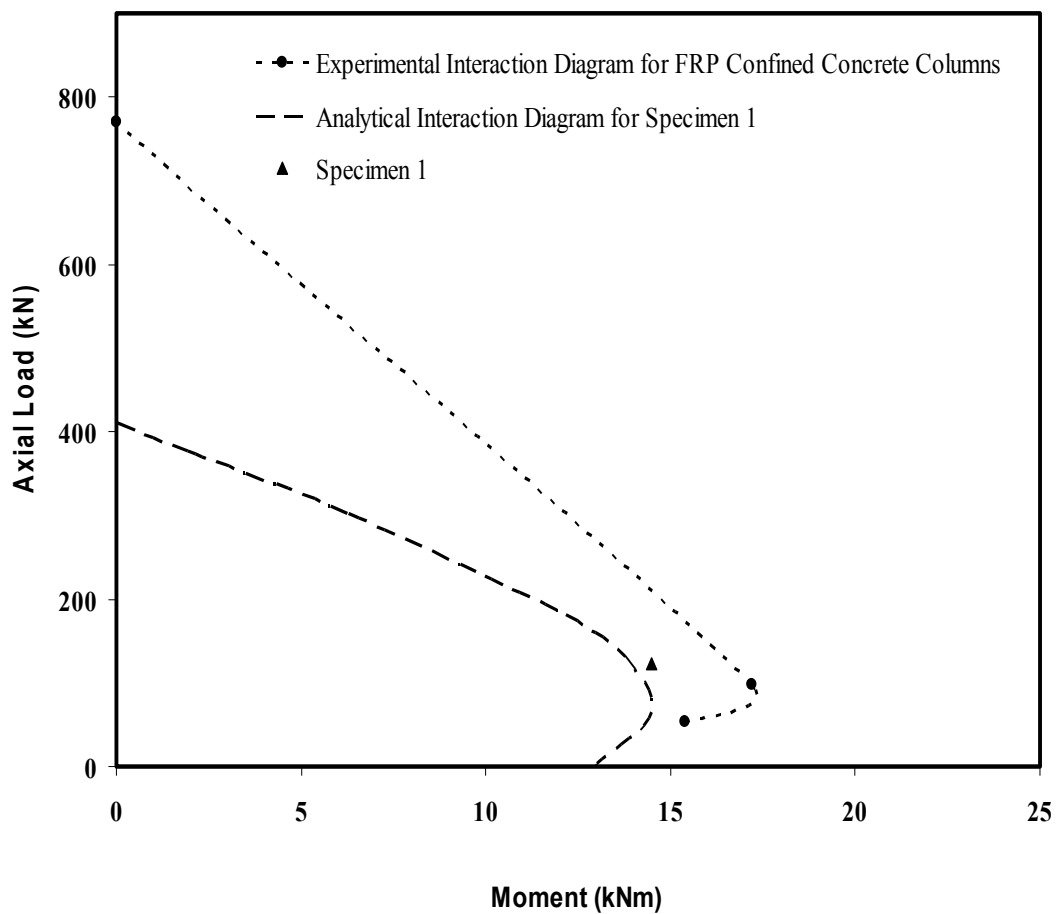


**Figure 2.6** Interaction Diagrams

In order to observe the confining stress distribution within the compression zone, strain measurements were taken around the FRP jacket along the perimeter

of Specimen 3 as it is shown in Figure 2.7. It was observed that ultimate curvature was reached at a maximum lateral strain of about 0.0085 at the extreme compression fiber. Results of strain measurements ( $\epsilon$ ) are used to obtain confinement ratio ( $\frac{E_f \epsilon t}{f'_c R}$  where  $E_f$  is the modulus of elasticity of FRP,  $t$  is the fiber thickness,  $R$  is the radius of column and  $f'_c$  is concrete compressive strength) are shown in Figure 2.7 with respect to gauge locations. It can be observed that confining stress distribution exhibited a nonlinear profile with the maximum occurring at the extreme compression fiber. The reason for this distribution can be attributed to the non-uniform axial strain distribution in the compression zone (usually assumed linear following Euler Bernoulli beam theory) and bond between the jacket and concrete resulting in a loss of confinement close to the neutral axis.

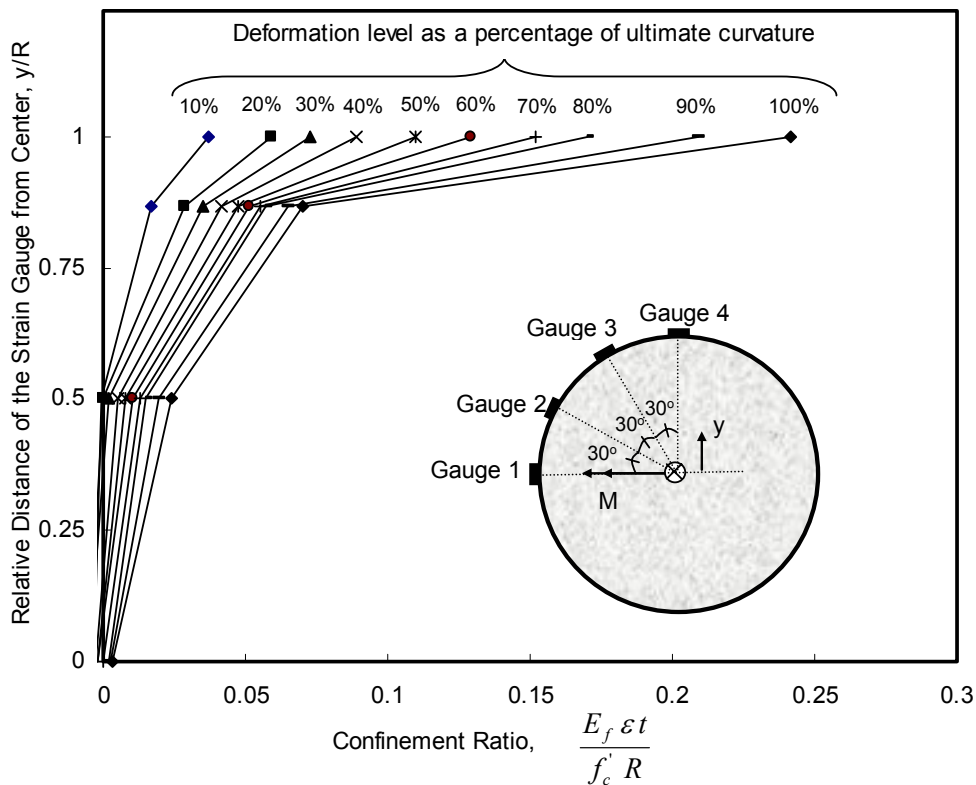


**Figure 2.7** Confining Stress Distribution for Specimen 3

## CHAPTER 3

### MODELING AND PARAMETRIC STUDIES

In this chapter, a new FRP confined concrete model is proposed and the results obtained from this model are compared with the results of the experimental study described in Chapter 2 and from study of Sheikh and Yau [13]. Finally, results of the parametric study are presented for 384 circular columns. An equation to estimate curvature ductility calibrated according to the results of the analyses of the columns is presented.

#### 3.1. FRP CONFINED CONCRETE MODEL DESCRIPTION

As mentioned in the first chapter, there are many studies on FRP confined concrete behavior. Most of these models are empirical in nature and employ best fit expressions as a function of the jacket properties to the experimentally obtained stress-strain curves. As pointed out by Xiao and Wu [4] and Wu et. al. [18], these models are calibrated only for FRP wrapped concrete that exhibits a hardening behavior. However, for large diameter bridge columns it is not always feasible to design for such confining pressures with low modulus FRPs. Hence, simple models that are capable of representing FRP confined concrete behavior ranging from softening to hardening response for different lateral pressures are needed. In this study, it was aimed to consider the effects of the confinement ratio so that hardening and softening response of the FRP confined column can be modeled. The proposed model can be applied for both circular and rectangular columns through well-established confinement efficiency factors.

As it is mentioned in the first chapter, the main factor that affects the stress and the ductility of a FRP confined concrete, is the amount of the lateral confining pressure. Increasing the lateral confining pressure increases both strength and the ductility. The non-dimensional confinement ratio can be computed as:

For circular columns:

$$\Phi = \frac{E_j \varepsilon_f t_j}{R f_c'}$$

For rectangular and square columns:

$$\Phi = \frac{(b+h)E_j \varepsilon_f t_j}{b h f_c'} K_e$$

where

$$K_e = 1 - \frac{(h-2r)^2 + (b-2r)^2}{3bh}$$

(3.1)

where

$E_j$  = elasticity modulus of FRP in the hoop direction

$\varepsilon_f$  = rupture strain of FRP jacket in the hoop direction

$t_j$  = thickness of the FRP jacket

$f_c'$  = unconfined concrete compressive strength

$R$  = radius of the confined concrete section

$b$  = width of the confined concrete cross section

$h$  = height of the confined concrete cross section

$r$  = radius of the rounded corner of the column

$K_e$  = effectiveness factor

For the sake of completeness, in Equation 3.1 the confinement ratio is also presented for rectangular columns as well.

The first important aspect of the FRP confined concrete model is the value of the confinement ratio at which behavior of the FRP confined concrete changes from softening to hardening. This value, named as transition value ( $\Phi_t$ ), is between 0.1 and 0.15 in the references [12], [18] and [19]. In this study this value is chosen as 0.14, (based on available test results shown in Figure 3.2), meaning

when the confinement ratio is smaller than the 0.14, softening behavior is observed and when the confinement ratio is larger than the 0.14, hardening behavior is expected in the stress-strain response.

The stress-strain curve of FRP confined concrete can be described with a non-linear first region and a straight line second region. The ultimate compressive strength and the ultimate axial strain of the FRP confined concrete define the end of the second portion of the curve. As it is shown in Figure 3.1a and Figure 3.1b if softening occurs, the second portion of the curve is a descending linear line and if hardening occurs the second portion is an ascending linear line. Initial slope of the curve is independent of the FRP confinement and it is equal to elasticity modulus of the concrete,  $E_c$ , ( $E_c = 4750\sqrt{f'_c}$  according to ACI and  $E_c = 3250\sqrt{f_{ck}} + 14000$  in (MPa) according to TS-500, where  $f_{ck}$  is the characteristic concrete strength). There is a breaking point of the curves which occurs at the point  $(\varepsilon_{co}, f'_c)$ .  $\varepsilon_{co}$ , which is the strain of the peak stress of an unconfined concrete, is expressed in Equation 3.2 which is defined by Taşdemir et. al. [20]. The ultimate strength ( $f'_{cu}$ ) and the ultimate strain ( $\varepsilon_{cu}$ ) is obtained by multiplying the unconfined concrete compressive strength ( $f'_c$ ) and the axial strain  $\varepsilon_{co}$  by the residual strength and strain enhancement factors ( $K_\sigma$  and  $K_\varepsilon$ ) respectively. In this way, the initial  $(\varepsilon_{co}, f'_c)$  and end point  $(f'_{cu}, \varepsilon_{cu})$ , which are used to express the equation of the second portion of the stress-strain curve, can be obtained using Equations 3.2 to 3.4:

$$\varepsilon_{co} = (-0.067f_c'^2 + 29.9f'_c + 1053)10^{-6} \quad (3.2)$$

$$f'_{cu} = K_\sigma f'_c \quad (3.3)$$

$$\varepsilon_{cu} = K_\varepsilon \varepsilon_{co} \quad (3.4)$$

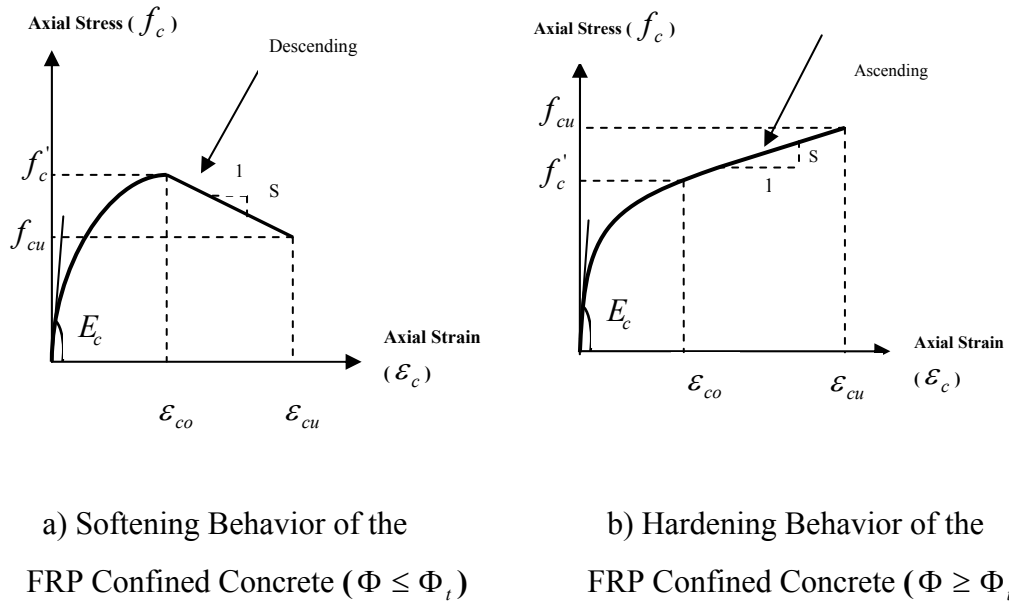


**Figure 3.1** FRP Confined Concrete Model

The residual strength enhancement factors ( $K_\sigma$ ) of hardening and softening are compared with the results presented in Lam and Teng [12], Xia and Wu [4], Wu et. al.[18] and Rochette and Labossiere [21] (Figure 3.2). When proposed equations of the residual strength enhancement factors ( $K_\sigma$ ) (explained in detail in the upcoming pages) are plotted onto these data, it can be seen that the test data are well represented by these equations of residual strength enhancement factor. It is also seen that when the confinement ratio is equal to the transition value 0.14,  $K_\sigma$  is 1.

The strain enhancement factor,  $K_\epsilon$ , is taken as proposed by Lam and Teng [12] obtained from the calibration of the 76 confined concrete specimens exhibiting both softening and hardening.

The proposed equations of the enhancement factors and the equations of the stress-strain behavior of the CFRP confined concrete with respect to softening and hardening are explained next.

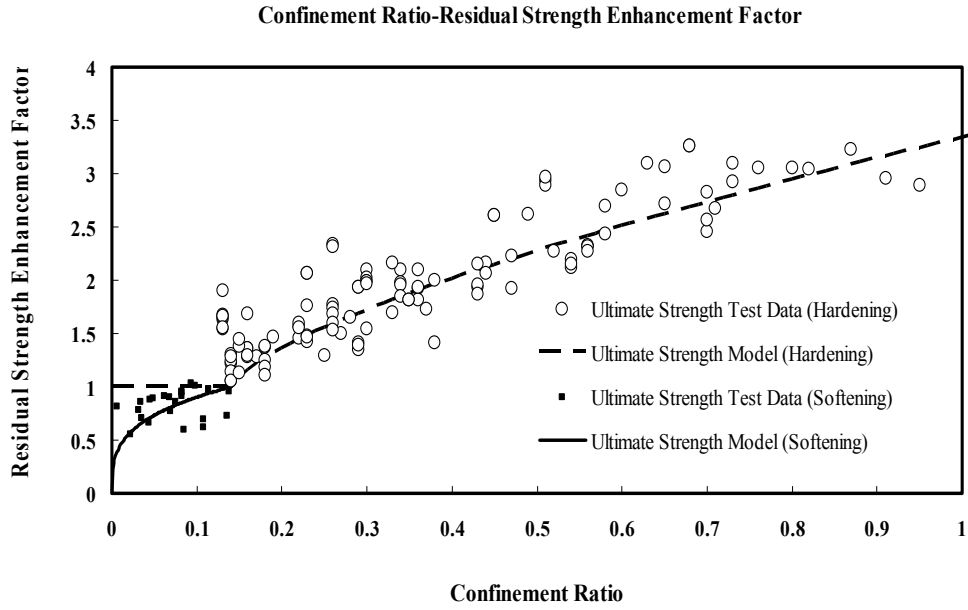


**Figure 3.2** Comparison of the Stress Enhancement Factors of Softening and Hardening Behavior of the FRP Confined Concrete

**In the case of softening ( $\Phi \leq \Phi_l$ ):**

$$K_\sigma = 1.8\Phi^{0.3} \quad (3.5)$$

$$K_\varepsilon = 1.75 + 12\Phi \left( \frac{\varepsilon_f}{\varepsilon_{co}} \right)^{0.45} \quad (3.6)$$

Hosotani and Kawashima [22] stated four boundary conditions for the stress-strain curve of the softening FRP confined concrete model. At the initial point of the curve there are two boundary conditions. The first one is  $f_c = 0$  at  $\varepsilon = 0$  and the second one is  $\frac{df_c}{d\varepsilon} = E_c$  at  $\varepsilon = 0$ . The third and fourth boundary conditions are at the peak point of the curve. The peak stress is equal to the unconfined concrete compressive strength ( $f'_c$ ) at  $\varepsilon = \varepsilon_{co}$  ( $\varepsilon_{co}$  is given in

Equation 3.2) and slope at peak stress  $\frac{df_c}{d\varepsilon} = 0$  at  $\varepsilon = \varepsilon_{co}$ .  $f_c$  is the compressive stress and  $\varepsilon$  is the axial strain of the FRP confined concrete in the study.

The stress of the first region ( $0 < \varepsilon < \varepsilon_{co}$ ) of the stress-strain curve is assumed as;

$$f_c = C_1 \varepsilon^n + C_2 \varepsilon + C_3 \quad (3.7)$$

where  $C_1$ ,  $C_2$ ,  $C_3$  and  $n$  are the constants which are obtained from the boundary condition of the equation so:

$$f_c = E_c \varepsilon \left[ 1 - \frac{1}{n} \left( \frac{\varepsilon}{\varepsilon_{co}} \right)^{n-1} \right] \quad 0 \leq \varepsilon \leq \varepsilon_{co} \quad (3.8)$$

where

$$n = \frac{E_c \varepsilon_{co}}{E_c \varepsilon_{co} - f'_c} \quad (3.9)$$

The second portion is a descending line when softening occurs. The slope ( $S$ ) of the line is:

$$S = \frac{(K_\sigma - 1)f'_c}{(K_\varepsilon - 1)\varepsilon_{co}} \quad (3.10)$$

$K_\sigma$  and  $K_\varepsilon$  for  $\Phi < \Phi_t$  is put into Equation 3.10.

And the stress-strain curve is given as:

$$f_c = f'_c + S(\varepsilon - \varepsilon_{co}) \quad \varepsilon \geq \varepsilon_{co} \quad (3.11)$$

or,

$$f_c = f'_c + \frac{(K_\sigma - 1)f'_c}{(K_\varepsilon - 1)\varepsilon_{co}} (\varepsilon - \varepsilon_{co}) \quad \varepsilon \geq \varepsilon_{co} \quad (3.12)$$

**In the case of hardening ( $\Phi \geq \Phi_t$ ):**

$$K_\sigma = 2.6(\Phi - 0.14)^{0.17} + 1 \quad (3.13)$$

$$K_\varepsilon = 1.75 + 12\Phi \left( \frac{\varepsilon_f}{\varepsilon_{co}} \right)^{0.45} \quad (3.6)$$

Similarly  $K_\sigma$  for the hardening curve is obtained with a nonlinear curve that satisfies  $K_\sigma = 0$  at  $\Phi = 0$  and  $K_\sigma = 1$  at  $\Phi = \Phi_t$ . Same  $K_\varepsilon$  value as in Equation 3.6 is employed for the hardening curve.

Hosotani and Kawashima [22] argued that the slope at peak stress boundary condition in hardening behavior was only different boundary condition from the softening behavior. The other three conditions are the same as the ones mentioned in the softening behavior. In hardening behavior the slope at peak stress is  $\frac{df_c}{d\varepsilon} = S$  at  $\varepsilon = \varepsilon_{co}$  where  $S$  is the slope of the ascending line in the second portion. The same procedure of the softening behavior is applied to the hardening behavior and the constants ( $C_1$ ,  $C_2$ ,  $C_3$  and  $n$ ) are obtained using these boundary conditions. The stress equation of the first region is expressed as:

$$f_c = E_c \varepsilon \left[ 1 - \frac{1}{n} \left( 1 - \frac{S}{E_c} \right) \left( \frac{\varepsilon}{\varepsilon_{co}} \right)^{n-1} \right] \quad 0 \leq \varepsilon \leq \varepsilon_{co} \quad (3.14)$$

where

$$n = \frac{(E_c - S)\varepsilon_{co}}{E_c \varepsilon_{co} - f'_c} \quad (3.15)$$

$$S = \frac{(K_\sigma - 1)f'_c}{(K_\varepsilon - 1)\varepsilon_{co}} \quad (3.10)$$

$K_\sigma$  and  $K_\varepsilon$  for  $\Phi \geq \Phi_t$  is put into Equation 3.10.

The second portion is an ascending line when hardening occurs and by using the slope of the line the stress equation of the second portion is:

$$f_c = f_c' + S(\varepsilon - \varepsilon_{co}) \quad \varepsilon \geq \varepsilon_{co} \quad (3.11)$$

or,

$$f_c = f_c' + \frac{(K_\sigma - 1)f_c'}{(K_\varepsilon - 1)\varepsilon_{co}}(\varepsilon - \varepsilon_{co}) \quad \varepsilon \geq \varepsilon_{co} \quad (3.16)$$

When the confinement ratio is equal to the transition value (0.14 in this study), the second portion of the stress-strain behavior is a constant horizontal line at  $f_c = f_c'$  and this line continues up to the rupture strain ( $\varepsilon_{cu}$ ). The ultimate stress equations of the both softening and hardening behavior satisfy this condition of  $\Phi = \Phi_t$ . Hence, when confinement ratio is equal to the transition value, the stress-strain behavior of the FRP confined concrete is a nonlinear curve followed by a perfect plastic region.

The proposed model can be used to describe unconfined concrete behavior as well. Initial slope of the curve, the stress and the strain at the peak points in the first region are valid for unconfined concrete. The ultimate axial strain is defined as  $1.75 \varepsilon_{co}$  for the unconfined concrete in this model. Therefore, one important advantage of the model is its ability to define unconfined concrete behavior, FRP confined concrete behavior with a softening region for low confinement and FRP confined behavior with a hardening region for high confined ones.

### 3.2. VERIFICATION OF THE MODEL

In this section the verification of the proposed model is given. The proposed model is verified with two different studies. Classical sectional analysis procedures (i.e discretizing the section into layer and incrementally satisfying equilibrium for pre defined top fiber strain) were employed in all the analyses using Response 2000. For concrete in compression proposed FRP confined concrete model was used whereas no tensile strength was assumed. For steel reinforcement an elastic perfectly plastic response with a second order hardening region was specified.

### **3.2.1. Verification of the Model with Experimental Results from This Study**

The circular columns (Specimen 1, Specimen 2, Specimen 3 and Specimen 4) which are studied in the Chapter 2 were analyzed by defining the proposed model as the stress-strain behavior of FRP confined concrete. The moment-curvature relationships obtained from experimental and analytical study were compared.

The Specimen 1 was a control specimen which had no FRP confinement. The analytical and experimental results are shown in Figure 3.3. The yield and ultimate curvature values of the analytical and experimental results were similar. The moment capacity of the analytical estimation was about %10 higher than that obtained in the experimental result.

The second and third specimens had an eccentricity of 29 cm and 17.5 cm, respectively. As it is seen in Figure 3.4 and Figure 3.5 the behavior of experimental and analytical are similar. The ductility increases in both curves in the figures compared to the control specimen. The ductility factors and the ultimate moment capacities of the experimental results are slightly higher than those obtained using the proposed model which were about %6 and %10, respectively. Experimental result of the Specimen 2 showed an ultimate moment capacity of about 18.00 kNm and a ductility factor of about 15 whereas the analytical solution had a moment capacity of about 16.50 kNm with a ductility factor of about 16.

### MOMENT-CURVATURE OF THE SPECIMEN 1

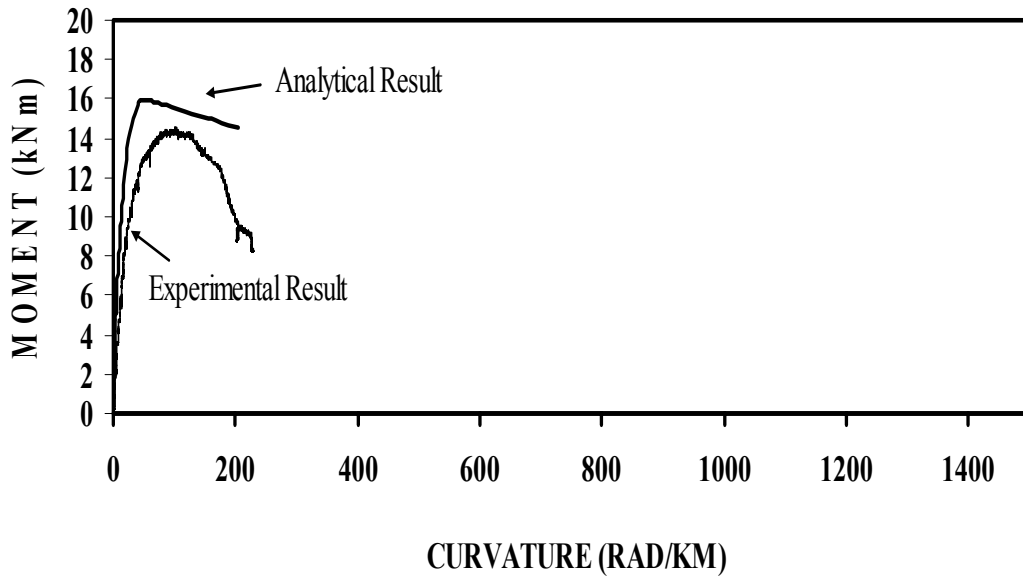


**Figure 3.3** Comparison of the Moment-Curvature Relationship of Specimen 1 with respect to Experimental and Analytical Study

The Specimen 3 had an experimental ultimate capacity and ductility factor of 20.50 kNm and 12, respectively. On the other side, the analytical moment capacity of the Specimen 3 was about 18.70 kNm with a ductility of 13. Also it can be seen that as the eccentricity decreases the ductility decreases as well. The FRP rupture (failure) occurred at the ultimate moment capacities both for experimental and analytical results.

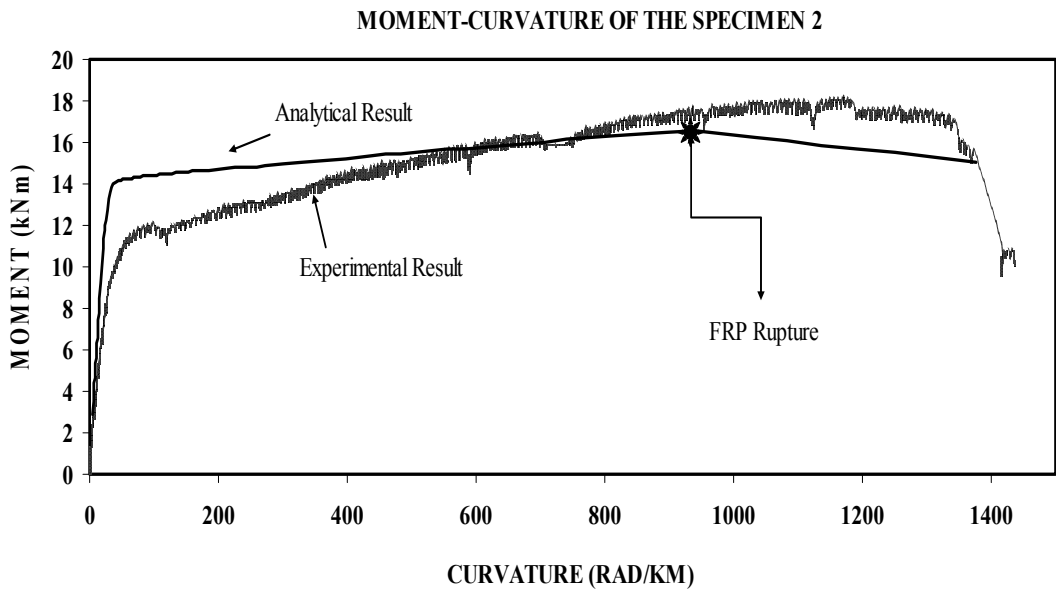


**Figure 3.4** Comparison of the Moment-Curvature Relationship of Specimen 2 with respect to Experimental and Analytical Study

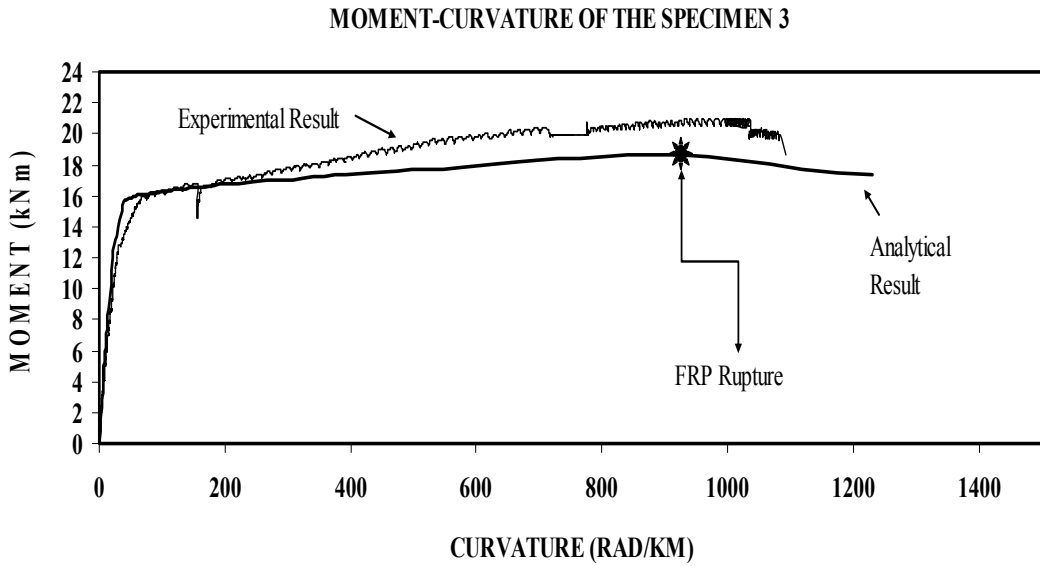


**Figure 3.5** Comparison of the Moment-Curvature Relationship of Specimen 3 with respect to Experimental and Analytical Study

Specimen 4 which was axially loaded had no bending moments. The load strain comparison is given in Figure 3.6. The axial strains of the specimen were measured by two strain and dial gages in the experimental study. The average of these experimental readings was plotted in the figure as strain gage and dial gage readings. As it is seen in the figure, the analytical results which exhibit a bilinear response as the experimental results agree well with dial gage and strain gage readings up to the yielding. After yielding, the analytical results show higher deformation than the experimental results as the load increases. This can be caused by the local nature of the strain gages' readings. Also it was thought that some accidental eccentricity might have occurred in the experiment while loading the specimen concentrically under compression so the analytical result of the specimen with a 1.5 cm eccentricity is also given. It can be said that the axial load carrying capacity of the specimen with  $e=1.5$  cm is similar to those observed in the experiment.

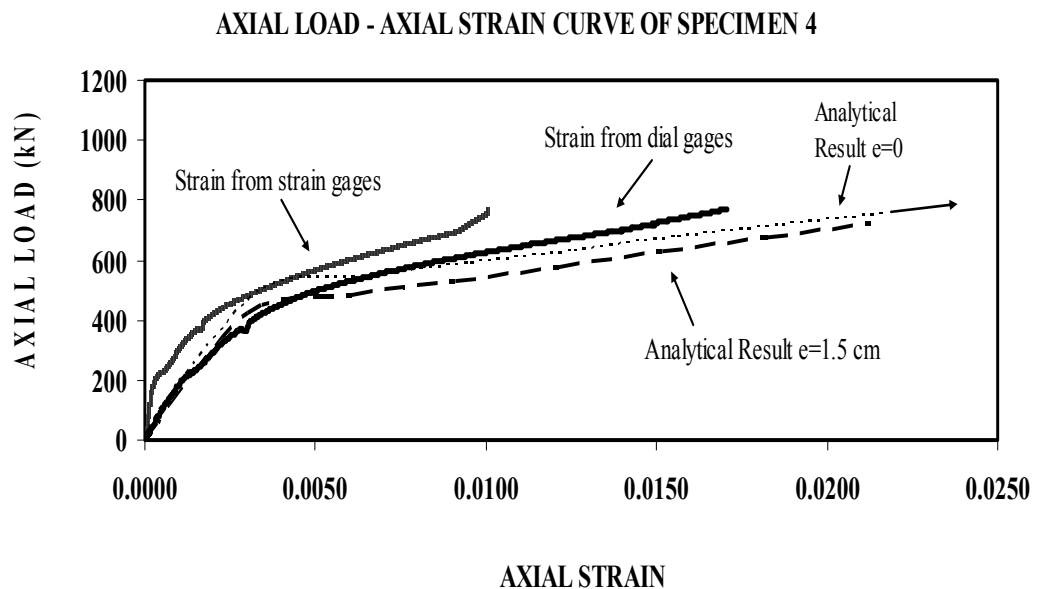


**Figure 3.6** Comparison of the Axial Load- Axial Strain Relationship of Specimen 4 with respect to Experimental and Analytical Study

### 3.2.2. Verification of the Model with the Paper of Sheikh and Yau [13]

As mentioned in Chapter 1, Sheikh and Yau [13] examined the effect of GFRP and CFRP wrapping on the behavior of circular columns by an experimental study. In their study, authors presented the moment-curvature results of the test specimens. These specimens were analyzed using the proposed model in this study and the obtained moment-curvature relationships are presented along with the results of the Sheikh and Yau [13] for the verification of the proposed model.

Each column had a 356 mm diameter with a length of 1.47 m and a stub of 510 x 760 x 810 mm. The clear cover of the specimens was 20 mm. The longitudinal bars were distributed through the circumference of the circular columns. All columns had six 25M longitudinal bars with the spirals which were U.S. No.3. The properties of the columns, FRP wrappings and reinforcement steel in the study of Sheikh and Yau [13] are listed in the Table 3.1, Table 3.2 and Table 3.3, respectively.

**Table 3.1** Properties of the Columns in the Paper of Sheikh and Yau [13]

Specimen	Lateral Reinforcement			FRP	Axial Load Ratio P/Po	$f'_c$ (MPa)
	Size	Spacing (mm)	$\rho_s$			
S-3NT	US No.3	300	0.30	No FRP	0.54	39.2
S-4NT	US No.3	300	0.30	No FRP	0.27	39.2
ST-2NT	US No.3	300	0.30	1.25 mm GFRP	0.54	40.4
ST-3NT	US No.3	300	0.30	1.00 mm CFRP	0.54	40.4
ST-4NT	US No.3	300	0.30	0.50 mm CFRP	0.27	44.8
ST-5NT	US No.3	300	0.30	1.25 mm GFRP	0.27	40.8

**Table 3.2** Properties of the FRP Composites in the Paper of Sheikh and Yau [13]

Name of the FRP	$t_j$	$E_j$	$\varepsilon_{ju}$
CFRP	0.5 mm	79166	0.0120
CFRP	1 mm	80952	0.0125
GFRP	1.25 mm	25641	0.0195

**Table 3.3** Properties of the Reinforcement Steel in the Paper of Sheikh and Yau [13]

Diameter	Yielding Stress (MPa)	Ultimate Stress (MPa)	Yielding Strain	Hardening Strain	Rupture Strain
25M	493	693	0.005	0.0275	0.1176
U.S No.3	506	786	0.005	0.0175	0.1294

The moment-curvature relationships obtained from analytical study are given in the Figure 3.7 and Figure 3.8 along with the envelope curves from the experimental study [13]. It is seen that the increase in the ductility with FRP jacketing is estimated with a reasonable engineering accuracy. As it is seen from the related figures, the strength and deformation capacity from experimental results and the analytical estimation agree well except specimens ST-4NT and ST-5NT for which curvature capacities are underestimated.

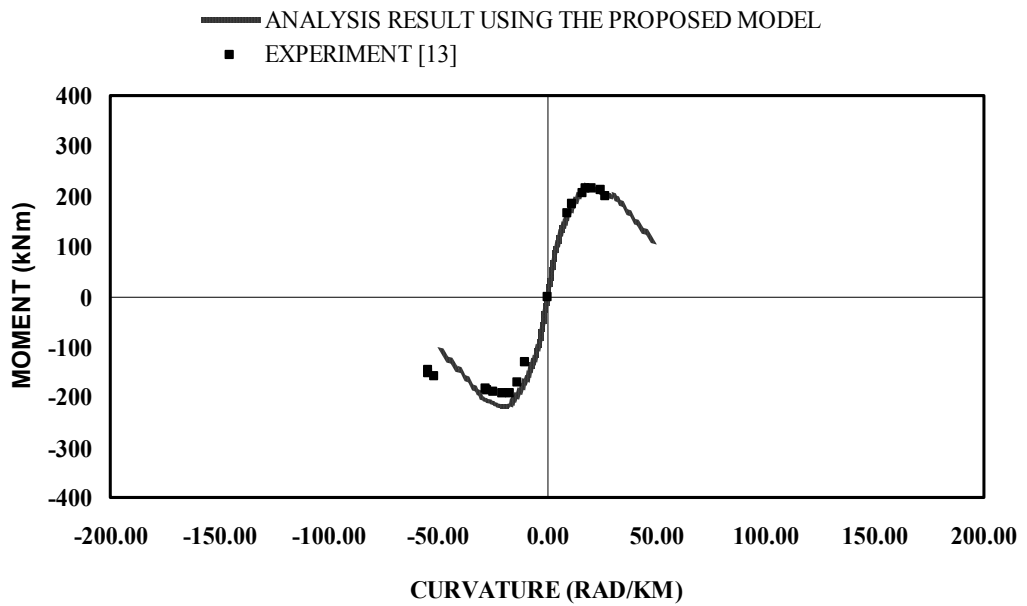
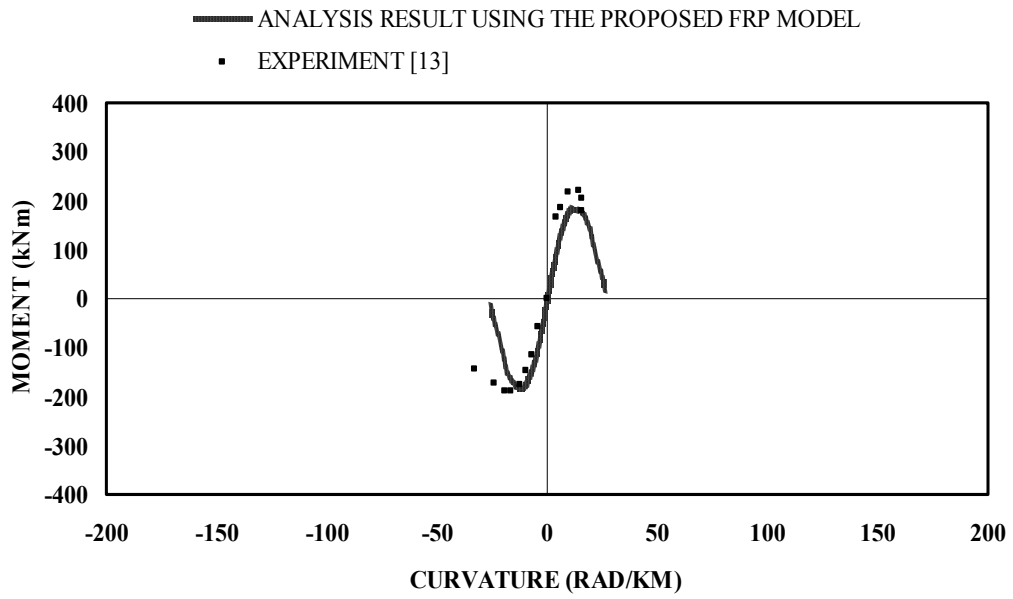


**Figure 3.7** Comparison of the Moment-Curvature Relationships of the Unconfined Specimens with respect to Paper [13] and Analytical Study

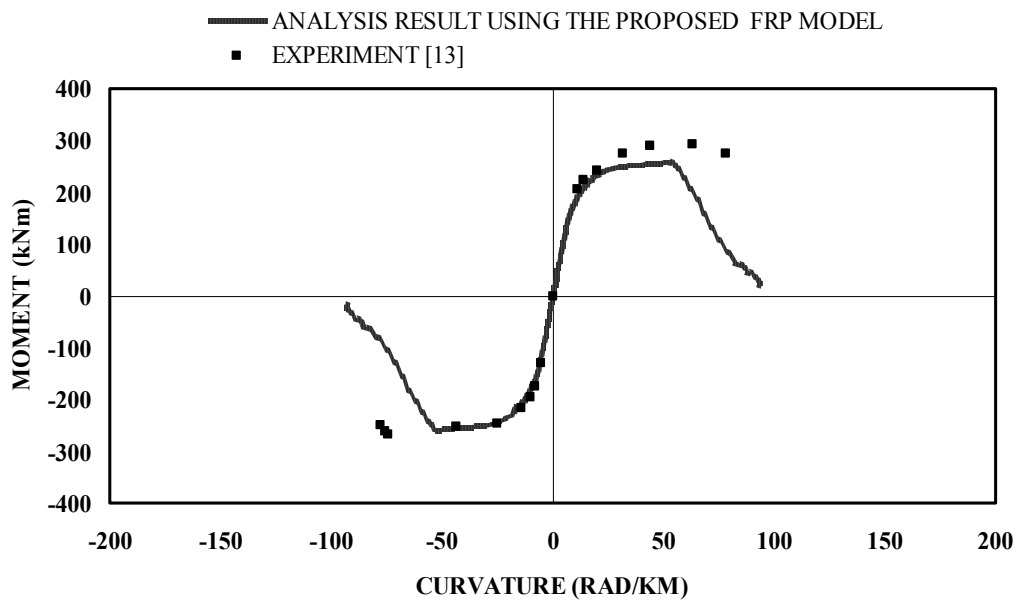
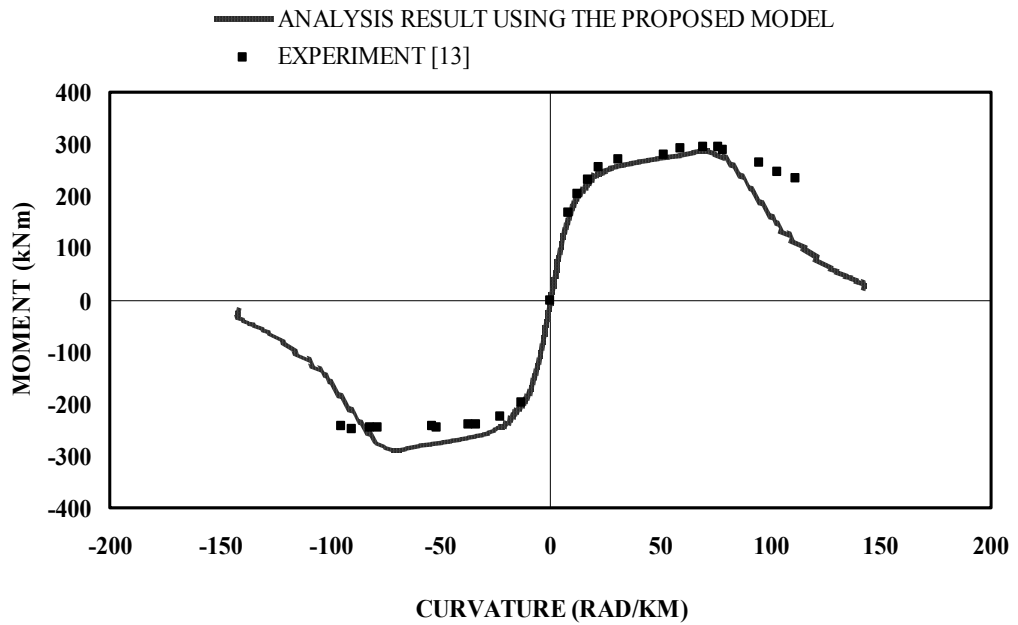


**Figure 3.8** Comparison of the Moment-Curvature Relationships of the FRP Confined Specimens with respect to Paper [13] and Analytical Study

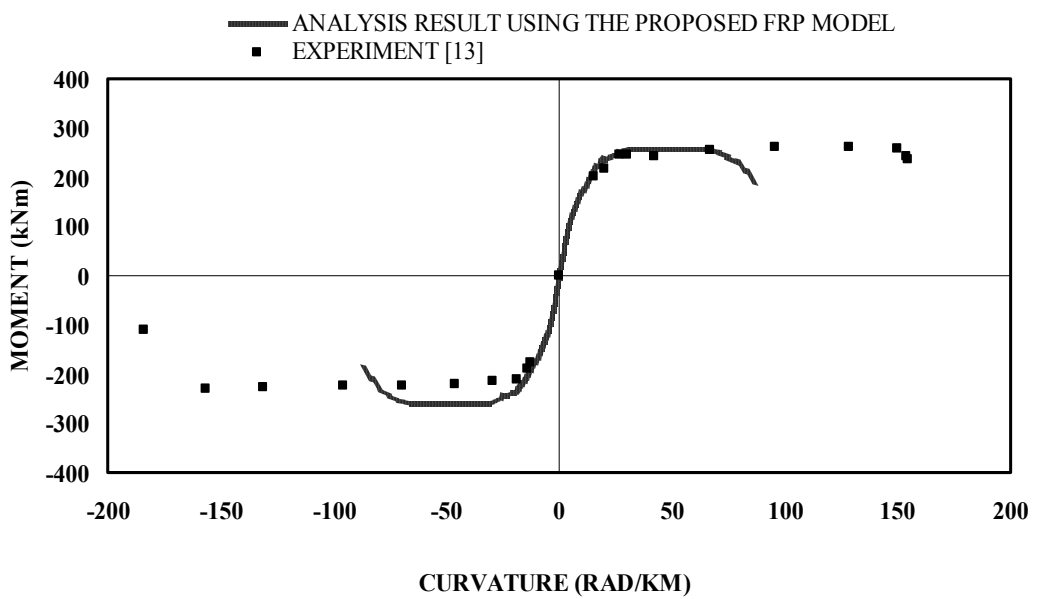
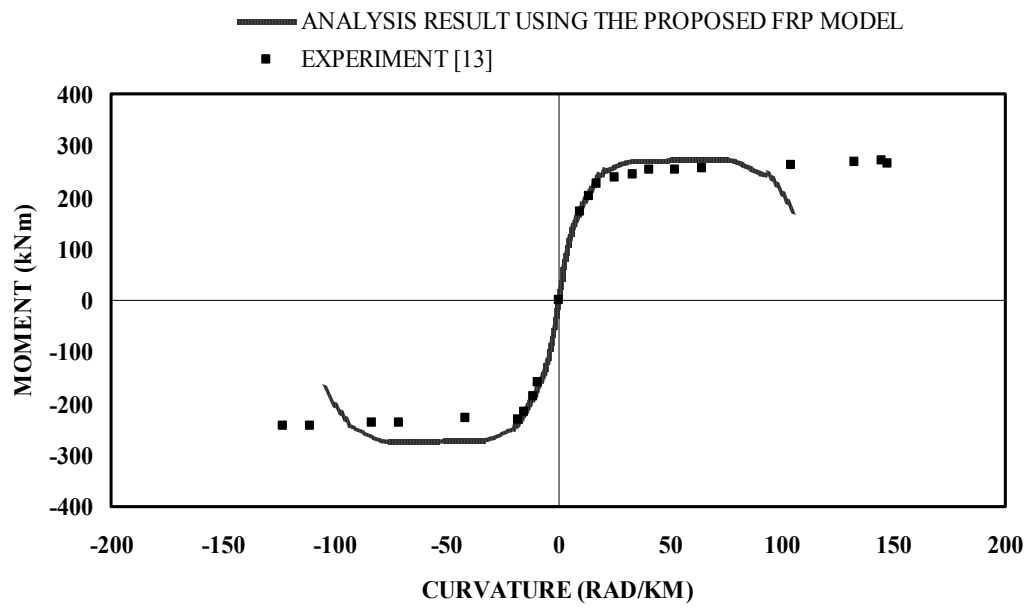


**Figure 3.8 (Cont'd)** Comparison of the Moment-Curvature Relationships of the FRP Confined Specimens with respect to Paper [13] and Analytical Study

As a result of these two verification studies of the proposed model, it can be said that the results of the proposed model are acceptable and the axial stress-strain model for FRP confined concrete under compression can reasonably be used to simulate experimental results.

### 3.3. PARAMETRIC STUDIES

In this part of the section, a parametric study was conducted to obtain an equation to estimate the curvature ductility factor of the CFRP wrapped circular columns using the proposed FRP confined concrete model. Taking the values of column diameter, concrete strength, longitudinal reinforcement ratio, axial load ratio and thickness of the CFRP confinement as analysis parameters, 384 different circular columns were designed with transverse reinforcement deficiency. Proposed analytical model was used as the CFRP wrapped concrete model of the columns. Moment-curvature relationships and the curvature ductility factors of the each column were obtained. Using the results of curvature ductilities and column parameters, an equation for the curvature ductility factor was obtained by regression analysis. The curvature ductility factor of each column was also calculated by this new equation and compared with the ductility factors obtained numerically with sectional analysis.

$$\text{Axial load ratio } (\eta = \frac{N}{f'_c A_g}), \text{ longitudinal reinforcement ratio } (\rho = \frac{A_s}{A_g}),$$

unconfined concrete compressive strength ( $f'_c$ ), diameter of the columns ( $D$ ) and the thickness of the CFRP wrapping ( $t_j$ ) were the main parameters of the study. It is possible to say that unconfined compressive concrete strength, diameter of the column and thickness of the wrapping can affect the confinement ratio ( $\Phi$ ). The confinement ratio is directly proportional with elasticity modulus ( $E_j$ ), rupture strain ( $\varepsilon_f$ ) of the CFRP and thickness of the CFRP ( $t_j$ ) and inversely with the radius of the confined concrete section ( $R$ ) and unconfined compressive concrete strength ( $f'_c$ ), (Equation 3.1). In addition to  $\Phi$ , axial load ratio ( $\eta$ ), longitudinal reinforcement ratio ( $\rho$ ) and the confinement ratio ( $\Phi$ ) are the three main

parameters which affect the curvature ductility factor of the CFRP wrapped circular columns.

The material properties of the steel and CFRP are constant for all columns. The steel used in the study as reinforcement, had a yield strength of 420 MPa with an elasticity modulus of 200000 MPa. The hardening strain and the rupture strain of the steel were 0.01 and 0.1 respectively. The elasticity modulus ( $E_j$ ) of the CFRP were 200000 Mpa with a rupture strain ( $\epsilon_f$ ) of 0.015. These properties of the steel and CFRP are shown in Table 3.4 and Table 3.5 respectively.

**Table 3.4** Material Properties of the Reinforcement Steel

<b>Material Properties of the Reinforcement Steel</b>	
Yielding Strength	420 MPa
Yielding Strain	0.0021
Hardening Strain	0.01
Rupture Strain	0.1

**Table 3.5** Material Properties of the CFRP

<b>Material Properties of the CFRP</b>	
Elasticity Modulus	200000 MPa
Rupture Strain	0.015

In the study there were three different column diameters which were 500 mm, 1000 mm and 2000 mm with the concrete cover of 20 mm, 30 mm and 40 mm, respectively. 384 different columns were designed by using the values of the parameters listed in Table 3.6. The concrete strength of the columns was 15 and

30 MPa. Longitudinal reinforcement ratios ( $\rho$ ) of the columns were selected as %1, %2, %3 and %4 and axial load ratios were 0.1, 0.2, 0.3 and 0.4. The diameters of the longitudinal reinforcements were between 14 mm and 56.4 mm according to the distribution of the reinforcement through the circumference of the circular column. The number of FRP layers was 0, 1, 2 and 3. The values of the confinement ratio ( $\Phi$ ) were varied between 0.1 and 2.4 as a result of the CFRP properties.

**Table 3.6** Details of Analysis

<b>Name of Parameters</b>	<b>Range of Parameters</b>
Diameter of the Longitudinal Reinforcement	Varies between $\phi$ 14 and $\phi$ 56
Uniaxial Compressive Strength of the Concrete	15 Mpa and 30 Mpa
Diameter of the Columns	500 mm, 1000 mm, 2000 mm
Axial Load Ratios	0.1, 0.2, 0.3 and 0.4
Longitudinal Reinforcement Ratios	%1, %2, %3 and %4
Thickness of the CFRP Jacket	0 (no jacket), 1 mm, 2mm,3 mm
Confinement Ratio ( $\Phi$ )	Varies between 0.1 and 2.4

Using these parameters, 384 circular columns were analyzed. In this way curvature ductility factor for each column was obtained so that a relationship between curvature ductility factor and the parameters could be established.

In Figure 3.9 the analytical relationship between the curvature ductility factor and confinement ratio with respect to column diameters, axial load ratios and longitudinal reinforcement ratios is shown. It is seen that CFRP jackets increased curvature ductility factors of the columns significantly. The curvature ductility factor reaches up to about 30 which is about the 25 times of unconfined concrete columns’.

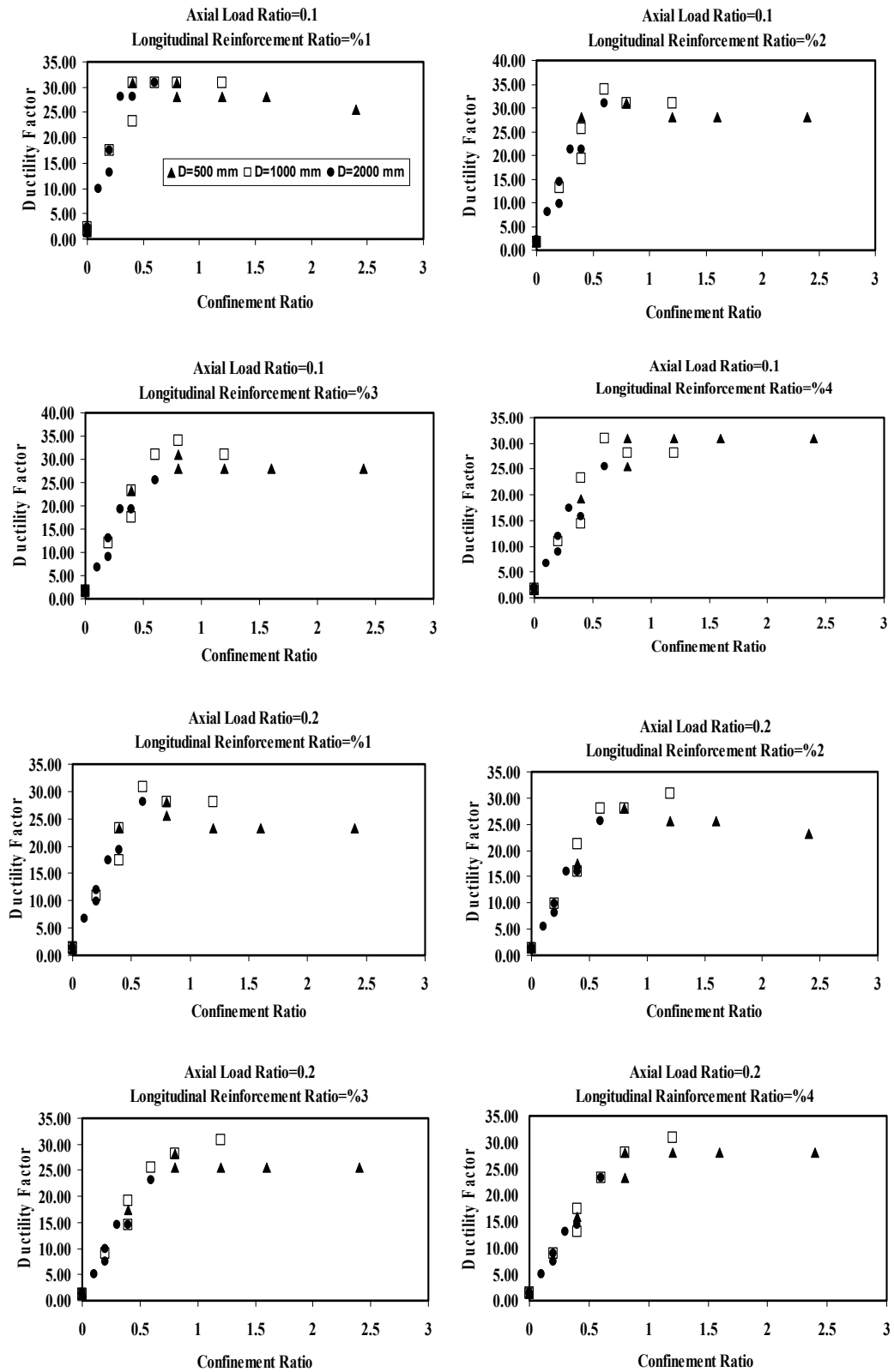


**Figure 3.9** Relationship between Ductility Factor and Confinement Ratio with respect to the Axial Load Ratio and Longitudinal Reinforcement Ratio

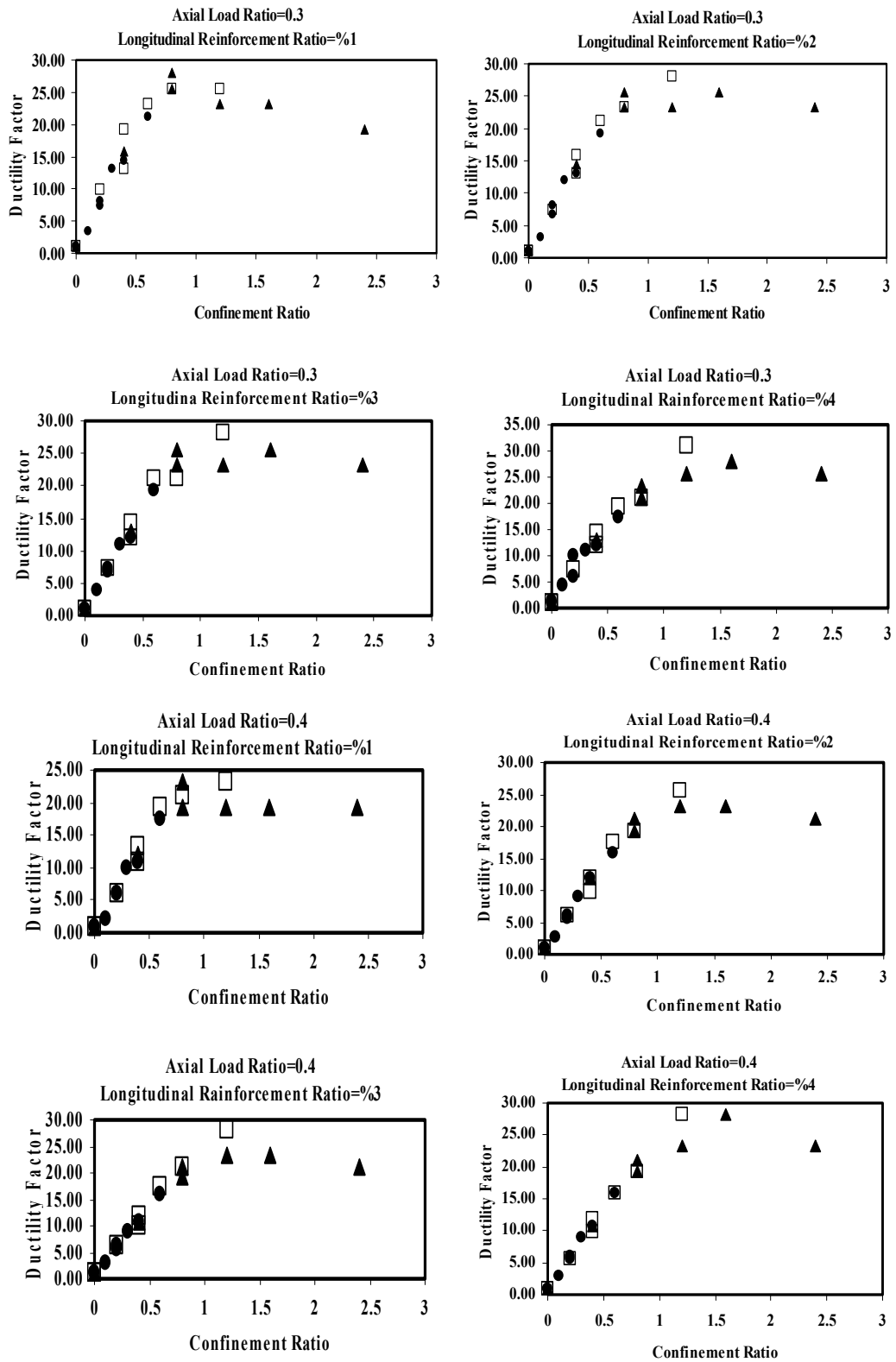


**Figure 3.9 (Cont'd)** Relationship between Ductility Factor and Confinement Ratio with respect to the Axial Load Ratio and Longitudinal Reinforcement Ratio

It can be observed that there is almost a linear relationship between curvature ductility factor and the confinement ratio up to the values at which reinforcing bar rupture occurs (Figure 3.9). With increasing thicknesses of the FRP jackets, bar rupture was observed instead of the FRP rupture because of the increased deformation demands. In Figure 3.9 it is also seen that when the bar rupture occurs the curvature ductility factors become approximately constant after a certain confinement ratio. It can be said that, a bi-linear relationship between curvature ductility factor and confinement ratio exists.

Under constant confinement ratio, the curvature ductility factor is inversely proportional with both axial load ratio and longitudinal reinforcement ratio. The Figure 3.10 shows the effect of axial load and longitudinal reinforcement ratios. As the axial load ratio increases under constant confinement ratio, the curvature ductility factor tends to decrease. Also, increasing longitudinal reinforcement ratio decreases the curvature ductility factor at low axial loads but the decrement caused by the axial load ratio is more pronounced. According to these results, the predictive equation of the ductility factor with respect to the confinement ratio can be represented with an equation in the form of:

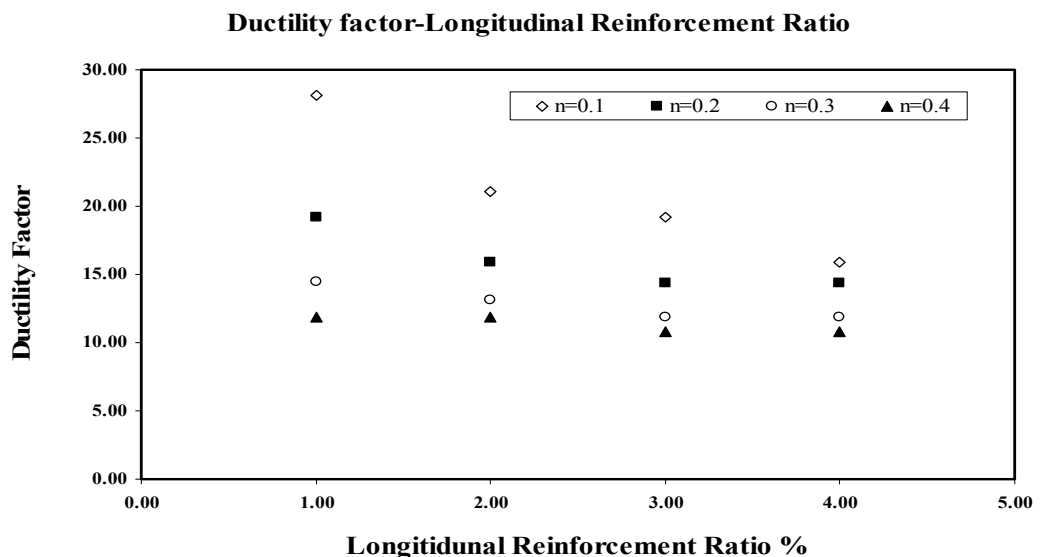


**Figure 3.10** Ductility Factor-Longitudinal Reinforcement and Axial Load Ratio  
For  $\Phi = 0.40$  and  $D = 2000$  mm

$$DF = S\Phi + K \leq DF_{\max} \quad (3.17)$$

where

$DF$  = curvature ductility factor

$S$  = slope of the equation

$\Phi$  = confinement ratio

$K$  = initial constant

$DF_{\max}$  = maximum ductility factor

The slope, initial constant and the maximum curvature ductility factor are three undetermined vales of the Equation 3.17. Since confinement ratio  $\Phi$  consists of the CFRP thickness, column diameter and the concrete strength; the slope and the initial constant of the equation should depend on the other parameters, namely axial load ratio and the longitudinal reinforcement ratio. Equation 3.17 can be divided into a linear line and constant line of  $DF_{\max}$ . The linear portion of the Equation 3.17 represents the columns with FRP rupture and constant line represents the columns with bar ruptures. Therefore Equation 3.17 in fact includes two different failure modes.

The average of the curvature ductility factors of the bar ruptures of columns is 27.0 which is considered as  $DF_{\max}$ .

A linear line was fitted onto the FRP rupture data of each graphic shown in Figure 3.9. In this way, the relationship between the curvature ductility factor and the confinement ratio was obtained under constant axial load ratio and longitudinal reinforcement ratio. The table of the slopes ( $S$ ) and initial constants ( $K$ ) of equations of these linear fits on the data of columns with FRP rupture is given in Table 3.7 for different axial load ratios and longitudinal reinforcement ratios.

**Table 3.7** List of the Slopes and Initial Constants of Equation of the  
Linear Fits on the Graphs of Figure 3.9

Model Parameters		Input Parameters	
Axial Load Ratio ( $\eta$ )	Longitudinal Reinforcement Ratio ( $\rho$ )	Slope ( $S$ )	Initial Constant ( $K$ )
0.1	0.01	62.86	1.92
0.1	0.02	55.32	1.78
0.1	0.03	46.20	1.70
0.1	0.04	36.67	1.65
0.2	0.01	49.06	1.34
0.2	0.02	38.42	1.34
0.2	0.03	35.47	1.30
0.2	0.04	30.84	1.36
0.3	0.01	36.20	1.00
0.3	0.02	30.32	1.03
0.3	0.03	28.87	1.03
0.3	0.04	27.54	1.10
0.4	0.01	26.00	1.00
0.4	0.02	24.61	1.00
0.4	0.03	24.82	1.00
0.4	0.04	23.64	1.00

The slope and the initial constant of the Equation 3.17 can be obtained by the determining the relationship of the slopes and initial constants of the equations in Table 3.7 as a function of axial load ratio ( $\eta$ ) and longitudinal reinforcement ratio ( $\rho$ ) separately. Therefore:

$$S = (2726\eta - 1130)\rho + (-152\eta + 86) \quad (3.18)$$

$$K = (33\eta - 9)\rho + (-3\eta + 2.10) \quad (3.19)$$

And the curvature ductility factor (Equation 3.17) becomes:

$$DF = [(2726\eta - 1130)\rho + (-152\eta + 86)]\Phi + (33\eta - 9)\rho + (-3\eta + 2.10) \leq 27 \quad (3.20)$$

The design parameters of each column of the study, failure types, curvature ductility factors, ratio of the curvature ductility factors with respect to analytical and parametric equation and moment capacity increments of the columns with respect to unconfined columns are shown in Appendix B. According to the analytical results, 24 % of the columns exhibited a bar rupture failure. When the failure types of the parametric equation examined, it is seen that only 4.5 % of the 384 columns show different failure type from the analytical failure types. The mean of the values of the ratio of the curvature ductility factor with respect to the analytical solution to the curvature ductility factor with respect to the parametric equation is 1.00 with a standard deviation of 0.13 which shows that the solutions of the parametric equation provides a good estimate of curvature ductility. In Figure 3.11 the ductility factors from the Equation 3.20 was plotted with respect to curvature ductility factors obtained from sectional analysis. The line which was fitted on the data passed as  $y = x$  which means ductility factors from Equation 3.20 and sectional analysis are very close to each other.

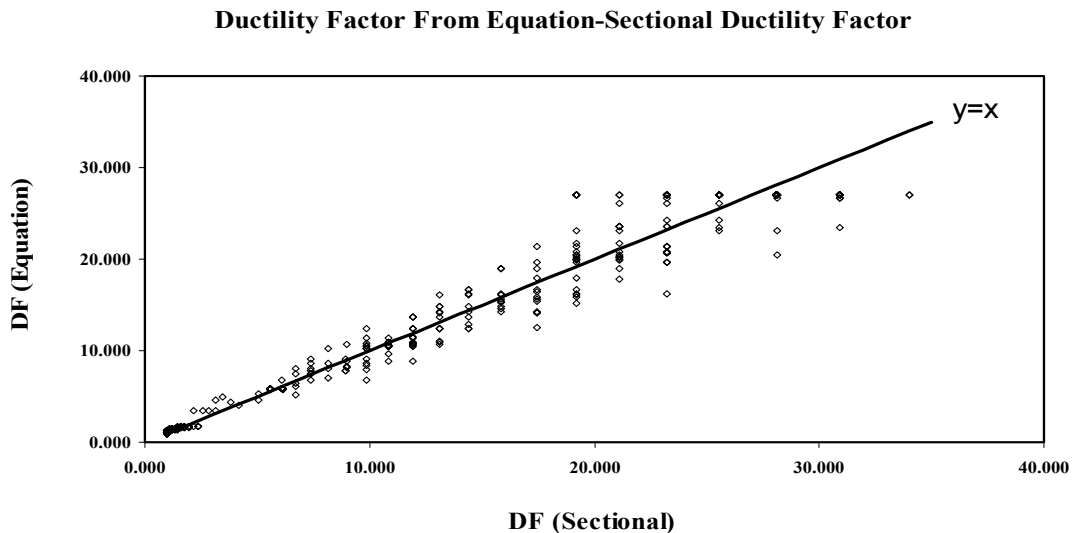


**Figure 3.11** Comparisons of the Ductility Factors from Equation 3.20 and Sectional Analysis

## CHAPTER 4

### CONCLUSION

This study presented an experimental and analytical study to show the effectiveness of the CFRP on the ductility of the circular columns which are designed for only gravity loads. An FRP confined concrete model was proposed and verified by comparing with experimental results from this study and the other research. Also a parametric study was conducted to obtain an equation for curvature ductility factor of FRP confined circular columns. The conclusions of the study are as follows:

1. In the experimental study, it was observed that CFRP wrapping increased the ductility of the columns significantly. Ductility factor of the control specimen increased from 2 to around 15. The energy dissipation and the deformation capacities and the deformations of the FRP confined columns were substantially higher than the column with no FRPs. According to the test results, it can be stated that as the eccentricity increases the ductility increases as well. The failure of all the FRP confined specimens in the experimental study was due to FRP rupture in a brittle and sudden manner.
2. Axial load bending moment interaction diagrams of the control specimen and FRP confined specimens were obtained using the test results. It was observed that the CFRP wrapping increased both axial load and bending moment capacities. Especially, the axial load capacity increases significantly for lower eccentricities.
3. The axial response of the CFRP confined concrete exhibited a bilinear behavior in the experimental study as well mentioned in the literature survey. The axial strain at the rupture was about 0.015, whereas the lateral strains were about 0.0085.

4. A nonlinear profile of the confining stress distribution was observed with the maximum occurring at the extreme compression fiber.
5. An axial stress-strain model in the form of Hosotani and Kawashima's [22] equation of FRP confined concrete was proposed. In this proposed model, the effects of the confinement ratio were taken into account and the FRP confined concrete behavior was defined with hardening and softening regions depending on the amount of the confinement ratio. The model is divided into two regions. The first region, which is a nonlinear curve, is same for hardening and softening responses. If the behavior is softening, the second region shows a descending line and if the behavior is hardening the second region shows an ascending line. The boundary conditions enabled to obtain a smooth transition from first region to second region of the behavior.
6. The proposed model was verified by comparing with the results of the experimental study and from the study by Sheikh and Yau [13]. It was observed that ductility factors and the ultimate moment capacities obtained from the model are about 6 to 10% higher than the results of the experimental study, respectively. For the axially loaded specimen, a bilinear response, similar to that obtained in the experiments, was observed. The situation of a small accidental eccentricity ( $e=1.5$  cm) was analyzed and it was observed that the estimate of axial load-deformation curve with this eccentricity was in good agreement with the experimental results. Also, the proposed model showed similar strength and deformation capacities with the results of the Sheikh and Yau [13] except two specimens for which curvature capacities were underestimated. Therefore, it can be concluded that the proposed model exhibits realistic and safe estimates and it can be used for determining the behavior of the FRP confined columns as a simple and useful model.
7. An equation of the curvature ductility factor for the circular columns was obtained as a result of the parametric study. It was observed that there is a

linear relationship between the curvature ductility factor and the confinement ratio up to the self-reinforcing bar rupture. Under constant confinement ratio the axial load ratio and the longitudinal reinforcement ratio is inversely proportional with the curvature ductility factor. As the axial load ratio or longitudinal reinforcement ratio increases the ductility factor decreases. It is proposed that the maximum ductility factor is 27 beyond which the longitudinal bar rupture occurs in the columns due to high strain demands. The ductility factors obtained from the equation was compared with the analytical ductility factors and it was found that the mean of the value of the ratio of the curvature ductility factor from the proposed equation to that obtained from sectional analysis was 1.00 with a standard deviation of 0.13. This shows that the proposed equation provides a good estimate of curvature ductility.

## REFERENCES

1. Mirmiran, A., Shahawy, M., Samaan, M., Echary, H.E., Mastrapa, J.C., and Pico, O., "Effect of Column Parameters on FRP Confined Concrete", *Journal of Composites for Construction*, Vol. 2, No. 4, November, 1998, pp 175-185.
2. Tan, K.H., "Strength Enhancement of Rectangular Reinforced Concrete Columns using Fiber-Reinforced Polymer", *Journal of Composites for Construction*, Vol. 6, No. 3, August 1, 2002, pp175-183.
3. Wang, Yung C. (Department of Civil Engineering, national Central University); Restrepo, Jose I., "Investigation of Concentrically Loaded Reinforced Concrete Columns Confined with Glass Fiber-Reinforced Polymer Jackets", *ACI Structural Journal*, Vol. 98, No. 3, May/June, 2001, pp 337-385.
4. Y. Xiao and H. Wu, "Compressive Behavior of Concrete Confined by Carbon Fiber Composite Jackets", *Journal of Materials in Civil Engineering*, Vol. 12, No. 2, May, 2000, pp 139-146.
5. İlki, A., and Kumbasar, N., "Compressive Behavior Carbon Fibre Composite Jacketed Concrete with Circular and Non-Circular Cross-Sections", *Journal of Earthquake Engineering*, Vol. 7, No. 3, 2003, pp 381-406.
6. Spoelstra, M.R., and Monti, G., "FRP-Confined Concrete Model", *Journal of Composites for Construction*, Vol. 3, No. 3, August, 1999, pp 143-150.
7. Mander, J.B., and Riestly, M.J.N., Park, R., "Theoretical Stress-Strain Model for Confined Concrete", *ASCE, Journal of Structural Engineering*, Vol. 114, No. 8, pp 1804-1826.

8. Popovics, Sandor, "Numerical Approach to the Complete Stress-Strain Relation for Concrete", *Cement and Concrete Research*, Vol. 3, No. 5, September, 1973, pp 583-599.
9. Pantazopoulou, S. J., and Mills, R. H., "Microstructural Aspects of the Mechanical Response of Plain Concrete", *ACI Mat. J.*, 92, November-December, 1995, pp 605-616.
10. Binici, B., "An Analytical Model for Stress-Strain Behavior of Confined Concrete", *Engineering Structures*, 27, 2005, pp 1040-1051.
11. Binici, B. and K.M. Mosalam, "Analysis of Reinforced Concrete Columns Retrofitted with Fiber Reinforced Polymer Lamina," *Composites Part B: Engineering*, in press and published online, 2006.
12. Lam, L., Teng, J.G., "Design-Oriented Stress-Strain Model for FRP-Confined Concrete", *Construction and Building Materials*, 17, 2003, pp 471-489.
13. Sheikh, S.A., Yau, G., "Seismic Behavior of Concrete Columns Confined with Steel and Fiber-Reinforced Polymers", *ACI Structural Journal*, Vol. 99, No. 1, January-February, 2002, pp 72-80.
14. Iacobucci, R.D., Sheikh, S.A., Bayrak, O., "Retrofit of Square Concrete Columns with Carbon Fiber-Reinforced Polymer for Seismic Resistance", *ACI Structural Journal*, Vol. 100, No. 6, November-December, 2003, pp 785-794.
15. Harajli, M.H., Rtwil, A.A., "Effect of Confinement Using Fiber Reinforced Polymer or Fiber-Reinforced Concrete on Seismic Performance of Gravity Load-Designed Columns", *ACI Structural Journal*, Vol. 101, No. 1, January-February, 2004, pp 47-56.
16. Seible, F., Priestley M.J.N., Hegemier, G.A., Innamorato, D., "Seismic Retrofit of RC Columns with Continuous Carbon Fiber Jackets", *Journal of Composites for Construction*, Vol. 1, No. 2, May, 1997, pp 52-62.

17. Çamlı Ü.S., “Anchorage Strength of Fiber Reinforced Polymers”, A Master of Sciences Thesis in Civil Engineering, Middle East Technical University, 2005.
18. Wu, G., Lu, Z.T., Wu, Z.S., “Strength and ductility of oncrete cylinders with FRP composites”, *Construction and Building Materials*, Vol. 20, No. 3, 2005, pp 134-148.
19. Mirmiran, A., Shahawy, M., Samaan, M., Echary, H.E., Masrapa, J.C., Pico, O., “Effect of Column Parameters on FRP-Confined Concrete”, *Journal of Composites for Construction*, Vol. 2, No. 4, 1998, pp 175-185.
20. Taşdemir, M.A., Taşdemir, C., Jefferson A.D., Lydon, F.D., Barr, B.I.G., “Evaluation of Strains at Peak Stresses in Concrete: A Three-Phase Composite Model Approach”, *Cement and Concrete Composites*, 20, 1998, pp 301-318.
21. Rochette, P., and Labossere, P., “Axial Testing of Rectangular Column Models Confined with Composites”, *Journal of Composites for Construction*, Vol. 4, No. 3, August, 2000, pp 129-136.
22. Hosotani, M. and Kawashima, K., “A Stress-Strain Model for Concrete Cylinders Confined by Both Carbon Fiber Sheets and Tie Reinforcement”, *Journal of Concrete Engineering*, JSCE 620/V-43, 1999, pp 25-42.
23. Baran M., “An Experimental Investigation on the Minimum Confinement Reinforcement Requirement of Spiral Columns”, A Master of Sciences Thesis in Civil Engineering, Middle East Technical University, 1999.
24. Dinçer S., “A Study on the Minimum Confinement in Spiral Columns”, A Master of Sciences Thesis in Civil Engineering, Middle East Technical University, 1999.

## APPENDIX A

### TABLE OF THE PARAMETRIC STUDY

The values of the parameters of the each column and results of the parametric study in the Chapter 3.3 are listed in Table B.1. In the table;

No = name of the column

n = number of the longitudinal bars

$D_b$  = diameter of the longitudinal bars in mm

$\rho$  = longitudinal reinforcement ratio in percentage

$\frac{N}{f_c' A_g}$  = axial load ratio

N = axial load in kN

$f_c'$  = concrete strength in MPa

$f_y$  = yielding strength in MPa

$D$  = diameter of the column in mm

$t_j$  = thickness of the CFRP jacket in mm

$\Phi$  = confinement ratio

$M_t / M_0$  = Ratio of the ultimate moment capacities of the CFRP confined column to the unconfined column

$DF$  = curvature ductility factor

$B / A$  = ratio of the curvature ductility factor obtained from computer analysis to the curvature ductility factor obtained from the parametric equation

The equation of the curvature ductility factor obtained as a result of the parametric study is;

$$DF = [(2726\eta - 1130)\rho + (-152\eta + 86)]\Phi + (33\eta - 9)\rho + (-3\eta + 2.10) \leq 27$$

**(3.20)**

**Table A.1** The Values of the Parameters of the Each Column and Results of the Parametric Study

No	n	$D_b$	$\rho$ %	$\frac{N}{f_c' A_g}$	N	$f_c'$	$f_y$	D	$t_j$	$\Phi$	$M_t / M_0$	DF wrt Parametric Equation (A)	DF From Computer Analysis (B)	B / A	Failure Mode with respect to Parametric Equation	Failure Mode with respect to Computer Analysis
1	13	14	1	0.1	-294.38	15	420	500	0	0	1.00	1.743	1.464	0.840	Concrete Failure	Concrete Failure
2	13	14	1	0.1	-294.38	15	420	500	1	1	1.47	27.000	28.102	1.041	Bar Rupture	Bar Rupture
3	13	14	1	0.1	-294.38	15	420	500	2	2	1.46	27.000	28.102	1.041	Bar Rupture	Bar Rupture
4	13	14	1	0.1	-294.38	15	420	500	3	2	1.46	27.000	25.547	0.946	Bar Rupture	Bar Rupture
5	25	20	1	0.1	-1177.50	15	420	1000	0	0	1.00	1.743	1.611	0.924	Concrete Failure	Concrete Failure
6	25	20	1	0.1	-1177.50	15	420	1000	1	0	1.33	26.633	23.226	0.872	FRP Rupture	FRP Rupture
7	25	20	1	0.1	-1177.50	15	420	1000	2	1	1.45	27.000	30.913	1.145	Bar Rupture	Bar Rupture
8	25	20	1	0.1	-1177.50	15	420	1000	3	1	1.45	27.000	30.913	1.145	Bar Rupture	Bar Rupture
9	51	28	1	0.1	-4710.00	15	420	2000	0	0	1.00	1.743	1.772	1.016	Concrete Failure	Concrete Failure
10	51	28	1	0.1	-4710.00	15	420	2000	1	0	1.19	14.188	13.111	0.924	FRP Rupture	FRP Rupture
11	51	28	1	0.1	-4710.00	15	420	2000	2	0	1.33	26.633	28.104	1.055	FRP Rupture	FRP Rupture
12	51	28	1	0.1	-4710.00	15	420	2000	3	1	1.41	27.000	30.915	1.145	Bar Rupture	FRP Rupture
13	13	14	1	0.1	-588.75	30	420	500	0	0	1.00	1.743	1.949	1.118	Concrete Failure	Concrete Failure
14	13	14	1	0.1	-588.75	30	420	500	1	0	1.33	26.633	30.915	1.161	FRP Rupture	FRP Rupture
15	13	14	1	0.1	-588.75	30	420	500	2	1	1.37	27.000	30.913	1.145	Bar Rupture	Bar Rupture
16	13	14	1	0.1	-588.75	30	420	500	3	1	1.37	27.000	28.102	1.041	Bar Rupture	Bar Rupture
17	25	20	1	0.1	-2355.00	30	420	1000	0	0	1.00	1.743	2.358	1.353	Concrete Failure	Concrete Failure

No	n	$D_b$	$\rho$ %	$\frac{N}{f_c' A_g}$	N	$f_c'$	$f_y$	D	$t_j$	$\Phi$	$M_t / M_0$	DF wrt Parametric Equation (A)	DF From Computer Analysis (B)	B / A	Failure Mode with respect to Parametric Equation	Failure Mode with respect to Computer Analysis
18	25	20	1	0.1	-2355.00	30	420	1000	1	0	1.18	14.188	17.452	1.230	FRP Rupture	FRP Rupture
19	25	20	1	0.1	-2355.00	30	420	1000	2	0	1.32	26.633	30.915	1.161	FRP Rupture	FRP Rupture
20	25	20	1	0.1	-2355.00	30	420	1000	3	1	1.33	27.000	30.915	1.145	Bar Rupture	Bar Rupture
21	51	28	1	0.1	-9420.00	30	420	2000	0	0	1.00	1.743	2.358	1.353	Concrete Failure	Concrete Failure
22	51	28	1	0.1	-9420.00	30	420	2000	1	0	1.08	7.966	9.851	1.237	FRP Rupture	FRP Rupture
23	51	28	1	0.1	-9420.00	30	420	2000	2	0	1.17	14.188	17.451	1.230	FRP Rupture	FRP Rupture
24	51	28	1	0.1	-9420.00	30	420	2000	3	0	1.25	20.411	28.104	1.377	FRP Rupture	FRP Rupture
25	13	14	1	0.2	-588.75	15	420	500	0	0	1.00	1.476	1.100	0.745	Concrete Failure	Concrete Failure
26	13	14	1	0.2	-588.75	15	420	500	1	1	1.54	27.000	28.102	1.041	Bar Rupture	Bar Rupture
27	13	14	1	0.2	-588.75	15	420	500	2	2	1.53	27.000	23.225	0.860	Bar Rupture	Bar Rupture
28	13	14	1	0.2	-588.75	15	420	500	3	2	1.54	27.000	23.225	0.860	Bar Rupture	Bar Rupture
29	25	20	1	0.2	-2355.00	15	420	1000	0	0	1.00	1.476	1.331	0.902	Concrete Failure	Concrete Failure
30	25	20	1	0.2	-2355.00	15	420	1000	1	0	1.36	21.377	17.449	0.816	FRP Rupture	FRP Rupture
31	25	20	1	0.2	-2355.00	15	420	1000	2	1	1.51	27.000	28.105	1.041	Bar Rupture	Bar Rupture
32	25	20	1	0.2	-2355.00	15	420	1000	3	1	1.51	27.000	28.105	1.041	Bar Rupture	Bar Rupture
33	51	28	1	0.2	-9420.00	15	420	2000	0	0	1.00	1.476	1.331	0.902	Concrete Failure	Concrete Failure
34	51	28	1	0.2	-9420.00	15	420	2000	1	0	1.21	11.426	9.850	0.862	FRP Rupture	FRP Rupture
35	51	28	1	0.2	-9420.00	15	420	2000	2	0	1.35	21.377	19.196	0.898	FRP Rupture	FRP Rupture
36	51	28	1	0.2	-9420.00	15	420	2000	3	1	1.47	27.000	28.100	1.041	Bar Rupture	Bar Rupture

No	n	$D_b$	$\rho$ %	$\frac{N}{f_c' A_g}$	N	$f_c'$	$f_y$	D	$t_j$	$\Phi$	$M_t / M_0$	DF wrt Parametric Equation (A)	DF From Computer Analysis (B)	B / A	Failure Mode with respect to Parametric Equation	Failure Mode with respect to Computer Analysis
37	13	14	1	0.2	-1177.50	30	420	500	0	0	1.00	1.476	1.331	0.902	Concrete Failure	Concrete Failure
38	13	14	1	0.2	-1177.50	30	420	500	1	0	1.30	21.377	23.225	1.086	FRP Rupture	FRP Rupture
39	13	14	1	0.2	-1177.50	30	420	500	2	1	1.38	27.000	25.547	0.946	Bar Rupture	Bar Rupture
40	13	14	1	0.2	-1177.50	30	420	500	3	1	1.38	27.000	23.225	0.860	Bar Rupture	Bar Rupture
41	25	20	1	0.2	-4710.00	30	420	1000	0	0	1.00	1.476	1.464	0.992	Concrete Failure	Concrete Failure
42	25	20	1	0.2	-4710.00	30	420	1000	1	0	1.17	11.426	10.835	0.948	FRP Rupture	FRP Rupture
43	25	20	1	0.2	-4710.00	30	420	1000	2	0	1.29	21.377	23.225	1.086	FRP Rupture	FRP Rupture
44	25	20	1	0.2	-4710.00	30	420	1000	3	1	1.37	27.000	30.913	1.145	Bar Rupture	Bar Rupture
45	51	28	1	0.2	-18840.00	30	420	2000	0	0	1.00	1.476	1.464	0.992	Concrete Failure	Concrete Failure
46	51	28	1	0.2	-18840.00	30	420	2000	1	0	1.07	6.451	6.728	1.043	FRP Rupture	FRP Rupture
47	51	28	1	0.2	-18840.00	30	420	2000	2	0	1.16	11.426	11.919	1.043	FRP Rupture	FRP Rupture
48	51	28	1	0.2	-18840.00	30	420	2000	3	0	1.23	16.402	17.448	1.064	FRP Rupture	FRP Rupture
49	13	14	1	0.3	-883.13	15	420	500	0	0	1.00	1.209	1.000	0.827	Concrete Failure	Concrete Failure
50	13	14	1	0.3	-883.13	15	420	500	1	1	1.71	27.000	28.102	1.041	Bar Rupture	Bar Rupture
51	13	14	1	0.3	-883.13	15	420	500	2	2	1.72	27.000	23.225	0.860	Bar Rupture	Bar Rupture
52	13	14	1	0.3	-883.13	15	420	500	3	2	1.71	27.000	19.194	0.711	Bar Rupture	Bar Rupture
53	25	20	1	0.3	-3532.50	15	420	1000	0	0	1.00	1.209	1.000	0.827	Concrete Failure	Concrete Failure
54	25	20	1	0.3	-3532.50	15	420	1000	1	0	1.45	16.120	13.111	0.813	FRP Rupture	FRP Rupture
55	25	20	1	0.3	-3532.50	15	420	1000	2	1	1.67	27.000	25.547	0.946	Bar Rupture	Bar Rupture

No	n	$D_b$	$\rho$ %	$\frac{N}{f_c' A_g}$	N	$f_c'$	$f_y$	D	$t_j$	$\Phi$	$M_t / M_0$	DF wrt Parametric Equation (A)	DF From Computer Analysis (B)	B / A	Failure Mode with respect to Parametric Equation	Failure Mode with respect to Computer Analysis
56	25	20	1	0.3	-3532.50	15	420	1000	3	1	1.67	27.000	25.547	0.946	Bar Rupture	Bar Rupture
57	51	28	1	0.3	-14130.00	15	420	2000	0	0	1.00	1.209	1.000	0.827	Concrete Failure	Concrete Failure
58	51	28	1	0.3	-14130.00	15	420	2000	1	0	1.28	8.665	7.399	0.854	FRP Rupture	FRP Rupture
59	51	28	1	0.3	-14130.00	15	420	2000	2	0	1.43	16.120	14.420	0.895	FRP Rupture	FRP Rupture
60	51	28	1	0.3	-14130.00	15	420	2000	3	1	1.55	23.576	21.112	0.896	FRP Rupture	FRP Rupture
61	13	14	1	0.3	-1766.25	30	420	500	0	0	1.00	1.209	1.000	0.827	Concrete Failure	Concrete Failure
62	13	14	1	0.3	-1766.25	30	420	500	1	0	1.38	16.120	15.863	0.984	FRP Rupture	FRP Rupture
63	13	14	1	0.3	-1766.25	30	420	500	2	1	1.52	27.000	25.547	0.946	Bar Rupture	Bar Rupture
64	13	14	1	0.3	-1766.25	30	420	500	3	1	1.52	27.000	23.225	0.860	Bar Rupture	Bar Rupture
65	25	20	1	0.3	-7065.00	30	420	1000	0	0	1.00	1.209	1.000	0.827	Concrete Failure	Concrete Failure
66	25	20	1	0.3	-7065.00	30	420	1000	1	0	1.22	8.665	9.850	1.137	FRP Rupture	FRP Rupture
67	25	20	1	0.3	-7065.00	30	420	1000	2	0	1.36	16.120	19.196	1.191	FRP Rupture	FRP Rupture
68	25	20	1	0.3	-7065.00	30	420	1000	3	1	1.47	23.576	23.225	0.985	FRP Rupture	FRP Rupture
69	51	28	1	0.3	-28260.00	30	420	2000	0	0	1.00	1.209	1.000	0.827	Concrete Failure	Concrete Failure
70	51	28	1	0.3	-28260.00	30	420	2000	1	0	1.10	4.937	3.452	0.699	FRP Rupture	FRP Rupture
71	51	28	1	0.3	-28260.00	30	420	2000	2	0	1.21	8.665	8.140	0.939	FRP Rupture	FRP Rupture
72	51	28	1	0.3	-28260.00	30	420	2000	3	0	1.29	12.392	13.109	1.058	FRP Rupture	FRP Rupture
73	13	14	1	0.4	-1177.50	15	420	500	0	0	1.00	0.942	1.000	1.062	Concrete Failure	Concrete Failure
74	13	14	1	0.4	-1177.50	15	420	500	1	1	1.91	20.785	19.194	0.923	FRP Rupture	FRP Rupture

No	n	$D_b$	$\rho$ %	$\frac{N}{f_c' A_g}$	N	$f_c'$	$f_y$	D	$t_j$	$\Phi$	$M_t / M_0$	DF wrt Parametric Equation (A)	DF From Computer Analysis (B)	B / A	Failure Mode with respect to Parametric Equation	Failure Mode with respect to Computer Analysis
75	13	14	1	0.4	-1177.50	15	420	500	2	2	1.97	27.000	19.194	0.711	Bar Rupture	Bar Rupture
76	13	14	1	0.4	-1177.50	15	420	500	3	2	1.98	27.000	19.194	0.711	Bar Rupture	Bar Rupture
77	25	20	1	0.4	-4710.00	15	420	1000	0	0	1.00	0.942	1.000	1.062	Concrete Failure	Concrete Failure
78	25	20	1	0.4	-4710.00	15	420	1000	1	0	1.62	10.864	10.835	0.997	FRP Rupture	FRP Rupture
79	25	20	1	0.4	-4710.00	15	420	1000	2	1	1.87	20.785	21.113	1.016	FRP Rupture	FRP Rupture
80	25	20	1	0.4	-4710.00	15	420	1000	3	1	1.94	27.000	23.223	0.860	Bar Rupture	Bar Rupture
81	51	28	1	0.4	-18840.00	15	420	2000	0	0	1.00	0.942	1.000	1.062	Concrete Failure	Concrete Failure
82	51	28	1	0.4	-18840.00	15	420	2000	1	0	1.41	5.903	6.116	1.036	FRP Rupture	FRP Rupture
83	51	28	1	0.4	-18840.00	15	420	2000	2	0	1.59	10.864	10.837	0.998	FRP Rupture	FRP Rupture
84	51	28	1	0.4	-18840.00	15	420	2000	3	1	1.73	15.824	17.452	1.103	FRP Rupture	FRP Rupture
85	13	14	1	0.4	-2355.00	30	420	500	0	0	1.00	0.942	1.000	1.062	Concrete Failure	Concrete Failure
86	13	14	1	0.4	-2355.00	30	420	500	1	0	1.53	10.864	11.918	1.097	FRP Rupture	FRP Rupture
87	13	14	1	0.4	-2355.00	30	420	500	2	1	1.75	20.785	23.225	1.117	FRP Rupture	Bar Rupture
88	13	14	1	0.4	-2355.00	30	420	500	3	1	1.75	27.000	19.194	0.711	Bar Rupture	Bar Rupture
89	25	20	1	0.4	-9420.00	30	420	1000	0	0	1.00	0.942	1.000	1.062	Concrete Failure	Concrete Failure
90	25	20	1	0.4	-9420.00	30	420	1000	1	0	1.32	5.903	6.116	1.036	FRP Rupture	FRP Rupture
91	25	20	1	0.4	-9420.00	30	420	1000	2	0	1.51	10.864	13.110	1.207	FRP Rupture	FRP Rupture
92	25	20	1	0.4	-9420.00	30	420	1000	3	1	1.63	15.824	19.194	1.213	FRP Rupture	FRP Rupture
93	51	28	1	0.4	-37680.00	30	420	2000	0	0	1.00	0.942	1.000	1.062	Concrete Failure	Concrete Failure

No	n	$D_b$	$\rho$ %	$\frac{N}{f_c' A_g}$	N	$f_c'$	$f_y$	D	$t_j$	$\Phi$	$M_t / M_0$	DF wrt Parametric Equation (A)	DF From Computer Analysis (B)	B / A	Failure Mode with respect to Parametric Equation	Failure Mode with respect to Computer Analysis
94	51	28	1	0.4	-37680.00	30	420	2000	1	0	1.17	3.422	2.144	0.626	FRP Rupture	FRP Rupture
95	51	28	1	0.4	-37680.00	30	420	2000	2	0	1.31	5.903	6.117	1.036	FRP Rupture	FRP Rupture
96	51	28	1	0.4	-37680.00	30	420	2000	3	0	1.43	8.383	9.851	1.175	FRP Rupture	FRP Rupture
97	15	18	2	0.1	-294.38	15	420	500	0	0	1.00	1.686	1.611	0.955	Concrete Failure	Concrete Failure
98	15	18	2	0.1	-294.38	15	420	500	1	1	1.58	27.000	30.912	1.145	Bar Rupture	Bar Rupture
99	15	18	2	0.1	-294.38	15	420	500	2	2	1.57	27.000	28.102	1.041	Bar Rupture	Bar Rupture
100	15	18	2	0.1	-294.38	15	420	500	3	2	1.57	27.000	28.102	1.041	Bar Rupture	Bar Rupture
101	30	26	2	0.1	-1177.50	15	420	1000	0	0	1.00	1.686	1.610	0.955	Concrete Failure	Concrete Failure
102	30	26	2	0.1	-1177.50	15	420	1000	1	0	1.35	23.147	19.196	0.829	FRP Rupture	FRP Rupture
103	30	26	2	0.1	-1177.50	15	420	1000	2	1	1.52	27.000	30.913	1.145	Bar Rupture	Bar Rupture
104	30	26	2	0.1	-1177.50	15	420	1000	3	1	1.52	27.000	30.913	1.145	Bar Rupture	Bar Rupture
105	62	36	2	0.1	-4710.00	15	420	2000	0	0	1.00	1.686	1.610	0.955	Concrete Failure	Concrete Failure
106	62	36	2	0.1	-4710.00	15	420	2000	1	0	1.19	12.416	9.850	0.793	FRP Rupture	FRP Rupture
107	62	36	2	0.1	-4710.00	15	420	2000	2	0	1.34	23.147	21.115	0.912	FRP Rupture	FRP Rupture
108	62	36	2	0.1	-4710.00	15	420	2000	3	1	1.46	27.000	30.915	1.145	Bar Rupture	Bar Rupture
109	15	18	2	0.1	-588.75	30	420	500	0	0	1.00	1.686	1.949	1.156	Concrete Failure	Concrete Failure
110	15	18	2	0.1	-588.75	30	420	500	1	0	1.35	23.147	28.104	1.214	FRP Rupture	FRP Rupture
111	15	18	2	0.1	-588.75	30	420	500	2	1	1.42	27.000	30.913	1.145	Bar Rupture	Bar Rupture
112	15	18	2	0.1	-588.75	30	420	500	3	1	1.41	27.000	28.102	1.041	Bar Rupture	Bar Rupture

No	n	$D_b$	$\rho$ %	$\frac{N}{f_c' A_g}$	N	$f_c'$	$f_y$	D	$t_j$	$\Phi$	$M_t / M_0$	DF wrt Parametric Equation (A)	DF From Computer Analysis (B)	B / A	Failure Mode with respect to Parametric Equation	Failure Mode with respect to Computer Analysis
113	30	26	2	0.1	-2355.00	30	420	1000	0	0	1.00	1.686	1.772	1.051	Concrete Failure	Concrete Failure
114	30	26	2	0.1	-2355.00	30	420	1000	1	0	1.17	12.416	13.111	1.056	FRP Rupture	FRP Rupture
115	30	26	2	0.1	-2355.00	30	420	1000	2	0	1.32	23.147	25.549	1.104	FRP Rupture	FRP Rupture
116	30	26	2	0.1	-2355.00	30	420	1000	3	1	1.40	27.000	34.006	1.259	Bar Rupture	Bar Rupture
117	62	36	2	0.1	-9420.00	30	420	2000	0	0	1.00	1.686	2.144	1.271	Concrete Failure	Concrete Failure
118	62	36	2	0.1	-9420.00	30	420	2000	1	0	1.08	7.051	8.141	1.155	FRP Rupture	FRP Rupture
119	62	36	2	0.1	-9420.00	30	420	2000	2	0	1.17	12.416	14.422	1.162	FRP Rupture	FRP Rupture
120	62	36	2	0.1	-9420.00	30	420	2000	3	0	1.25	17.782	21.115	1.187	FRP Rupture	FRP Rupture
121	15	18	2	0.2	-588.75	15	420	500	0	0	1.00	1.452	1.210	0.833	Concrete Failure	Concrete Failure
122	15	18	2	0.2	-588.75	15	420	500	1	1	1.62	27.000	28.102	1.041	Bar Rupture	FRP Rupture
123	15	18	2	0.2	-588.75	15	420	500	2	2	1.66	27.000	25.547	0.946	Bar Rupture	Bar Rupture
124	15	18	2	0.2	-588.75	15	420	500	3	2	1.66	27.000	23.225	0.860	Bar Rupture	Bar Rupture
125	30	26	2	0.2	-2355.00	15	420	1000	0	0	1.00	1.452	1.210	0.833	Concrete Failure	Concrete Failure
126	30	26	2	0.2	-2355.00	15	420	1000	1	0	1.38	19.014	15.863	0.834	FRP Rupture	FRP Rupture
127	30	26	2	0.2	-2355.00	15	420	1000	2	1	1.60	27.000	28.105	1.041	Bar Rupture	Bar Rupture
128	30	26	2	0.2	-2355.00	15	420	1000	3	1	1.61	27.000	30.916	1.145	Bar Rupture	Bar Rupture
129	62	36	2	0.2	-9420.00	15	420	2000	0	0	1.00	1.452	1.331	0.917	Concrete Failure	Concrete Failure
130	62	36	2	0.2	-9420.00	15	420	2000	1	0	1.22	10.233	8.139	0.795	FRP Rupture	FRP Rupture
131	62	36	2	0.2	-9420.00	15	420	2000	2	0	1.36	19.014	15.861	0.834	FRP Rupture	FRP Rupture

No	n	$D_b$	$\rho$ %	$\frac{N}{f_c' A_g}$	N	$f_c'$	$f_y$	D	$t_j$	$\Phi$	$M_t / M_0$	DF wrt Parametric Equation (A)	DF From Computer Analysis (B)	B / A	Failure Mode with respect to Parametric Equation	Failure Mode with respect to Computer Analysis
132	62	36	2	0.2	-9420.00	15	420	2000	3	1	1.47	27.000	25.545	0.946	Bar Rupture	FRP Rupture
133	15	18	2	0.2	-1177.50	30	420	500	0	0	1.00	1.452	1.464	1.008	Concrete Failure	Concrete Failure
134	15	18	2	0.2	-1177.50	30	420	500	1	0	1.34	19.014	17.449	0.918	FRP Rupture	FRP Rupture
135	15	18	2	0.2	-1177.50	30	420	500	2	1	1.49	27.000	28.102	1.041	Bar Rupture	Bar Rupture
136	15	18	2	0.2	-1177.50	30	420	500	3	1	1.49	27.000	25.547	0.946	Bar Rupture	Bar Rupture
137	30	26	2	0.2	-4710.00	30	420	1000	0	0	1.00	1.452	1.331	0.917	Concrete Failure	Concrete Failure
138	30	26	2	0.2	-4710.00	30	420	1000	1	0	1.19	10.233	9.850	0.963	FRP Rupture	FRP Rupture
139	30	26	2	0.2	-4710.00	30	420	1000	2	0	1.33	19.014	21.114	1.110	FRP Rupture	FRP Rupture
140	30	26	2	0.2	-4710.00	30	420	1000	3	1	1.44	27.000	28.105	1.041	Bar Rupture	Bar Rupture
141	62	36	2	0.2	-18840.00	30	420	2000	0	0	1.00	1.452	1.464	1.008	Concrete Failure	Concrete Failure
142	62	36	2	0.2	-18840.00	30	420	2000	1	0	1.09	5.842	5.559	0.952	FRP Rupture	FRP Rupture
143	62	36	2	0.2	-18840.00	30	420	2000	2	0	1.18	10.233	9.849	0.962	FRP Rupture	FRP Rupture
144	62	36	2	0.2	-18840.00	30	420	2000	3	0	1.26	14.623	15.861	1.085	FRP Rupture	FRP Rupture
145	15	18	2	0.3	-883.13	15	420	500	0	0	1.00	1.218	1.000	0.821	Concrete Failure	Concrete Failure
146	15	18	2	0.3	-883.13	15	420	500	1	1	1.72	27.000	23.225	0.860	Bar Rupture	FRP Rupture
147	15	18	2	0.3	-883.13	15	420	500	2	2	1.84	27.000	25.548	0.946	Bar Rupture	Bar Rupture
148	15	18	2	0.3	-883.13	15	420	500	3	2	1.83	27.000	23.226	0.860	Bar Rupture	Bar Rupture
149	30	26	2	0.3	-3532.50	15	420	1000	0	0	1.00	1.218	1.000	0.821	Concrete Failure	Concrete Failure
150	30	26	2	0.3	-3532.50	15	420	1000	1	0	1.45	14.880	13.111	0.881	FRP Rupture	FRP Rupture

No	n	$D_b$	$\rho$ %	$\frac{N}{f_c' A_g}$	N	$f_c'$	$f_y$	D	$t_j$	$\Phi$	$M_t / M_0$	DF wrt Parametric Equation (A)	DF From Computer Analysis (B)	B / A	Failure Mode with respect to Parametric Equation	Failure Mode with respect to Computer Analysis
151	30	26	2	0.3	-3532.50	15	420	1000	2	1	1.68	27.000	23.225	0.860	Bar Rupture	FRP Rupture
152	30	26	2	0.3	-3532.50	15	420	1000	3	1	1.76	27.000	28.102	1.041	Bar Rupture	Bar Rupture
153	62	36	2	0.3	-14130.00	15	420	2000	0	0	1.00	1.218	1.000	0.821	Concrete Failure	Concrete Failure
154	62	36	2	0.3	-14130.00	15	420	2000	1	0	1.28	8.049	6.727	0.836	FRP Rupture	FRP Rupture
155	62	36	2	0.3	-14130.00	15	420	2000	2	0	1.43	14.880	13.109	0.881	FRP Rupture	FRP Rupture
156	62	36	2	0.3	-14130.00	15	420	2000	3	1	1.55	21.712	19.193	0.884	FRP Rupture	FRP Rupture
157	15	18	2	0.3	-1766.25	30	420	500	0	0	1.00	1.218	1.000	0.821	Concrete Failure	Concrete Failure
158	15	18	2	0.3	-1766.25	30	420	500	1	0	1.40	14.880	14.421	0.969	FRP Rupture	FRP Rupture
159	15	18	2	0.3	-1766.25	30	420	500	2	1	1.62	27.000	25.547	0.946	Bar Rupture	Bar Rupture
160	15	18	2	0.3	-1766.25	30	420	500	3	1	1.62	27.000	23.225	0.860	Bar Rupture	Bar Rupture
161	30	26	2	0.3	-7065.00	30	420	1000	0	0	1.00	1.218	1.100	0.903	Concrete Failure	Concrete Failure
162	30	26	2	0.3	-7065.00	30	420	1000	1	0	1.24	8.049	7.401	0.919	FRP Rupture	FRP Rupture
163	30	26	2	0.3	-7065.00	30	420	1000	2	0	1.39	14.880	15.865	1.066	FRP Rupture	FRP Rupture
164	30	26	2	0.3	-7065.00	30	420	1000	3	1	1.51	21.712	21.113	0.972	FRP Rupture	FRP Rupture
165	62	36	2	0.3	-28260.00	30	420	2000	0	0	1.00	1.218	1.100	0.903	Concrete Failure	Concrete Failure
166	62	36	2	0.3	-28260.00	30	420	2000	1	0	1.12	4.634	3.138	0.677	FRP Rupture	FRP Rupture
167	62	36	2	0.3	-28260.00	30	420	2000	2	0	1.23	8.049	8.140	1.011	FRP Rupture	FRP Rupture
168	62	36	2	0.3	-28260.00	30	420	2000	3	0	1.31	11.465	11.918	1.039	FRP Rupture	FRP Rupture
169	15	18	2	0.4	-1177.50	15	420	500	0	0	1.00	0.984	1.000	1.016	Concrete Failure	Concrete Failure

No	n	$D_b$	$\rho$ %	$\frac{N}{f_c' A_g}$	N	$f_c'$	$f_y$	D	$t_j$	$\Phi$	$M_t / M_0$	DF wrt Parametric Equation (A)	DF From Computer Analysis (B)	B / A	Failure Mode with respect to Parametric Equation	Failure Mode with respect to Computer Analysis
170	15	18	2	0.4	-1177.50	15	420	500	1	1	1.90	20.510	19.194	0.936	FRP Rupture	FRP Rupture
171	15	18	2	0.4	-1177.50	15	420	500	2	2	2.06	27.000	23.226	0.860	Bar Rupture	Bar Rupture
172	15	18	2	0.4	-1177.50	15	420	500	3	2	2.04	27.000	21.113	0.782	Bar Rupture	Bar Rupture
173	30	26	2	0.4	-4710.00	15	420	1000	0	0	1.00	0.984	1.000	1.016	Concrete Failure	Concrete Failure
174	30	26	2	0.4	-4710.00	15	420	1000	1	0	1.60	10.747	9.850	0.916	FRP Rupture	FRP Rupture
175	30	26	2	0.4	-4710.00	15	420	1000	2	1	1.85	20.510	19.194	0.936	FRP Rupture	FRP Rupture
176	30	26	2	0.4	-4710.00	15	420	1000	3	1	1.97	27.000	25.547	0.946	Bar Rupture	Bar Rupture
177	62	36	2	0.4	-18840.00	15	420	2000	0	0	1.00	0.984	1.000	1.016	Concrete Failure	Concrete Failure
178	62	36	2	0.4	-18840.00	15	420	2000	1	0	1.39	5.866	5.559	0.948	FRP Rupture	FRP Rupture
179	62	36	2	0.4	-18840.00	15	420	2000	2	0	1.56	10.747	11.918	1.109	FRP Rupture	FRP Rupture
180	62	36	2	0.4	-18840.00	15	420	2000	3	1	1.69	15.629	15.866	1.015	FRP Rupture	FRP Rupture
181	15	18	2	0.4	-2355.00	30	420	500	0	0	1.00	0.984	1.000	1.016	Concrete Failure	Concrete Failure
182	15	18	2	0.4	-2355.00	30	420	500	1	0	1.54	10.747	11.918	1.109	FRP Rupture	FRP Rupture
183	15	18	2	0.4	-2355.00	30	420	500	2	1	1.79	20.510	21.114	1.029	FRP Rupture	FRP Rupture
184	15	18	2	0.4	-2355.00	30	420	500	3	1	1.86	27.000	23.226	0.860	Bar Rupture	Bar Rupture
185	30	26	2	0.4	-9420.00	30	420	1000	0	0	1.00	0.984	1.000	1.016	Concrete Failure	Concrete Failure
186	30	26	2	0.4	-9420.00	30	420	1000	1	0	1.35	5.866	6.116	1.043	FRP Rupture	FRP Rupture
187	30	26	2	0.4	-9420.00	30	420	1000	2	0	1.52	10.747	11.918	1.109	FRP Rupture	FRP Rupture
188	30	26	2	0.4	-9420.00	30	420	1000	3	1	1.66	15.629	17.449	1.116	FRP Rupture	FRP Rupture

No	n	$D_b$	$\rho$ %	$\frac{N}{f_c' A_g}$	N	$f_c'$	$f_y$	D	$t_j$	$\Phi$	$M_t / M_0$	DF wrt Parametric Equation (A)	DF From Computer Analysis (B)	B / A	Failure Mode with respect to Parametric Equation	Failure Mode with respect to Computer Analysis
189	62	36	2	0.4	-37680.00	30	420	2000	0	0	1.00	0.984	1.000	1.016	Concrete Failure	Concrete Failure
190	62	36	2	0.4	-37680.00	30	420	2000	1	0	1.20	3.425	2.594	0.757	FRP Rupture	FRP Rupture
191	62	36	2	0.4	-37680.00	30	420	2000	2	0	1.33	5.866	6.117	1.043	FRP Rupture	FRP Rupture
192	62	36	2	0.4	-37680.00	30	420	2000	3	0	1.43	8.306	8.956	1.078	FRP Rupture	FRP Rupture
193	15	22	3	0.1	-294.38	15	420	500	0	0	1.00	1.629	1.464	0.899	Concrete Failure	Concrete Failure
194	15	22	3	0.1	-294.38	15	420	500	1	1	1.59	27.000	30.912	1.145	Bar Rupture	Bar Rupture
195	15	22	3	0.1	-294.38	15	420	500	2	2	1.59	27.000	28.102	1.041	Bar Rupture	Bar Rupture
196	15	22	3	0.1	-294.38	15	420	500	3	2	1.59	27.000	28.102	1.041	Bar Rupture	Bar Rupture
197	33	30	3	0.1	-1177.50	15	420	1000	0	0	1.00	1.629	1.610	0.989	Concrete Failure	Concrete Failure
198	33	30	3	0.1	-1177.50	15	420	1000	1	0	1.33	19.660	17.450	0.888	FRP Rupture	FRP Rupture
199	33	30	3	0.1	-1177.50	15	420	1000	2	1	1.54	27.000	34.004	1.259	Bar Rupture	Bar Rupture
200	33	30	3	0.1	-1177.50	15	420	1000	3	1	1.57	27.000	30.916	1.145	Bar Rupture	Bar Rupture
201	63	44	3	0.1	-4710.00	15	420	2000	0	0	1.00	1.629	1.610	0.989	Concrete Failure	Concrete Failure
202	63	44	3	0.1	-4710.00	15	420	2000	1	0	1.19	10.645	8.955	0.841	FRP Rupture	FRP Rupture
203	63	44	3	0.1	-4710.00	15	420	2000	2	0	1.32	19.660	19.196	0.976	FRP Rupture	FRP Rupture
204	63	44	3	0.1	-4710.00	15	420	2000	3	1	1.43	27.000	25.545	0.946	Bar Rupture	FRP Rupture
205	15	22	3	0.1	-588.75	30	420	500	0	0	1.00	1.629	1.772	1.088	Concrete Failure	Concrete Failure
206	15	22	3	0.1	-588.75	30	420	500	1	0	1.35	19.660	23.225	1.181	FRP Rupture	FRP Rupture
207	15	22	3	0.1	-588.75	30	420	500	2	1	1.43	27.000	28.102	1.041	Bar Rupture	Bar Rupture

No	n	$D_b$	$\rho$ %	$\frac{N}{f_c' A_g}$	N	$f_c'$	$f_y$	D	$t_j$	$\Phi$	$M_t / M_0$	DF wrt Parametric Equation (A)	DF From Computer Analysis (B)	B / A	Failure Mode with respect to Parametric Equation	Failure Mode with respect to Computer Analysis
208	15	22	3	0.1	-588.75	30	420	500	3	1	1.43	27.000	28.102	1.041	Bar Rupture	Bar Rupture
209	33	30	3	0.1	-2355.00	30	420	1000	0	0	1.00	1.629	1.772	1.088	Concrete Failure	Concrete Failure
210	33	30	3	0.1	-2355.00	30	420	1000	1	0	1.18	10.645	11.919	1.120	FRP Rupture	FRP Rupture
211	33	30	3	0.1	-2355.00	30	420	1000	2	0	1.32	19.660	23.226	1.181	FRP Rupture	FRP Rupture
212	33	30	3	0.1	-2355.00	30	420	1000	3	1	1.44	27.000	30.913	1.145	Bar Rupture	Bar Rupture
213	63	44	3	0.1	-9420.00	30	420	2000	0	0	1.00	1.629	1.949	1.196	Concrete Failure	Concrete Failure
214	63	44	3	0.1	-9420.00	30	420	2000	1	0	1.09	6.137	6.728	1.096	FRP Rupture	FRP Rupture
215	63	44	3	0.1	-9420.00	30	420	2000	2	0	1.17	10.645	13.111	1.232	FRP Rupture	FRP Rupture
216	63	44	3	0.1	-9420.00	30	420	2000	3	0	1.25	15.152	19.196	1.267	FRP Rupture	FRP Rupture
217	15	22	3	0.2	-588.75	15	420	500	0	0	1.00	1.428	1.100	0.770	Concrete Failure	Concrete Failure
218	15	22	3	0.2	-588.75	15	420	500	1	1	1.62	27.000	25.547	0.946	Bar Rupture	FRP Rupture
219	15	22	3	0.2	-588.75	15	420	500	2	2	1.68	27.000	25.547	0.946	Bar Rupture	Bar Rupture
220	15	22	3	0.2	-588.75	15	420	500	3	2	1.69	27.000	25.548	0.946	Bar Rupture	Bar Rupture
221	33	30	3	0.2	-2355.00	15	420	1000	0	0	1.00	1.428	1.210	0.847	Concrete Failure	Concrete Failure
222	33	30	3	0.2	-2355.00	15	420	1000	1	0	1.37	16.650	14.421	0.866	FRP Rupture	FRP Rupture
223	33	30	3	0.2	-2355.00	15	420	1000	2	1	1.58	27.000	28.105	1.041	Bar Rupture	FRP Rupture
224	33	30	3	0.2	-2355.00	15	420	1000	3	1	1.64	27.000	30.916	1.145	Bar Rupture	Bar Rupture
225	63	44	3	0.2	-9420.00	15	420	2000	0	0	1.00	1.428	1.210	0.847	Concrete Failure	Concrete Failure
226	63	44	3	0.2	-9420.00	15	420	2000	1	0	1.23	9.039	7.399	0.819	FRP Rupture	FRP Rupture

No	n	$D_b$	$\rho$ %	$\frac{N}{f_c' A_g}$	N	$f_c'$	$f_y$	D	$t_j$	$\Phi$	$M_t / M_0$	DF wrt Parametric Equation (A)	DF From Computer Analysis (B)	B / A	Failure Mode with respect to Parametric Equation	Failure Mode with respect to Computer Analysis
227	63	44	3	0.2	-9420.00	15	420	2000	2	0	1.35	16.650	14.419	0.866	FRP Rupture	FRP Rupture
228	63	44	3	0.2	-9420.00	15	420	2000	3	1	1.46	24.262	23.223	0.957	FRP Rupture	FRP Rupture
229	15	22	3	0.2	-1177.50	30	420	500	0	0	1.00	1.428	1.464	1.025	Concrete Failure	Concrete Failure
230	15	22	3	0.2	-1177.50	30	420	500	1	0	1.35	16.650	17.449	1.048	FRP Rupture	FRP Rupture
231	15	22	3	0.2	-1177.50	30	420	500	2	1	1.51	27.000	28.102	1.041	Bar Rupture	Bar Rupture
232	15	22	3	0.2	-1177.50	30	420	500	3	1	1.50	27.000	25.547	0.946	Bar Rupture	Bar Rupture
233	33	30	3	0.2	-4710.00	30	420	1000	0	0	1.00	1.428	1.331	0.932	Concrete Failure	Concrete Failure
234	33	30	3	0.2	-4710.00	30	420	1000	1	0	1.19	9.039	8.954	0.991	FRP Rupture	FRP Rupture
235	33	30	3	0.2	-4710.00	30	420	1000	2	0	1.34	16.650	19.194	1.153	FRP Rupture	FRP Rupture
236	33	30	3	0.2	-4710.00	30	420	1000	3	1	1.46	24.262	25.550	1.053	FRP Rupture	FRP Rupture
237	63	44	3	0.2	-18840.00	30	420	2000	0	0	1.00	1.428	1.464	1.025	Concrete Failure	Concrete Failure
238	63	44	3	0.2	-18840.00	30	420	2000	1	0	1.10	5.234	5.054	0.966	FRP Rupture	FRP Rupture
239	63	44	3	0.2	-18840.00	30	420	2000	2	0	1.19	9.039	9.849	1.090	FRP Rupture	FRP Rupture
240	63	44	3	0.2	-18840.00	30	420	2000	3	0	1.26	12.845	14.419	1.123	FRP Rupture	FRP Rupture
241	15	22	3	0.3	-883.13	15	420	500	0	0	1.00	1.227	1.000	0.815	Concrete Failure	Concrete Failure
242	15	22	3	0.3	-883.13	15	420	500	1	1	1.72	26.054	23.225	0.891	FRP Rupture	FRP Rupture
243	15	22	3	0.3	-883.13	15	420	500	2	2	1.87	27.000	25.548	0.946	Bar Rupture	Bar Rupture
244	15	22	3	0.3	-883.13	15	420	500	3	2	1.85	27.000	23.226	0.860	Bar Rupture	Bar Rupture
245	33	30	3	0.3	-3532.50	15	420	1000	0	0	1.00	1.227	1.000	0.815	Concrete Failure	Concrete Failure

No	n	$D_b$	$\rho$ %	$\frac{N}{f_c' A_g}$	N	$f_c'$	$f_y$	D	$t_j$	$\Phi$	$M_t / M_0$	DF wrt Parametric Equation (A)	DF From Computer Analysis (B)	B / A	Failure Mode with respect to Parametric Equation	Failure Mode with respect to Computer Analysis
246	33	30	3	0.3	-3532.50	15	420	1000	1	0	1.44	13.641	11.919	0.874	FRP Rupture	FRP Rupture
247	33	30	3	0.3	-3532.50	15	420	1000	2	1	1.65	26.054	21.113	0.810	FRP Rupture	FRP Rupture
248	33	30	3	0.3	-3532.50	15	420	1000	3	1	1.76	27.000	28.102	1.041	Bar Rupture	Bar Rupture
249	63	44	3	0.3	-14130.00	15	420	2000	0	0	1.00	1.227	1.000	0.815	Concrete Failure	Concrete Failure
250	63	44	3	0.3	-14130.00	15	420	2000	1	0	1.28	7.434	6.727	0.905	FRP Rupture	FRP Rupture
251	63	44	3	0.3	-14130.00	15	420	2000	2	0	1.41	13.641	11.918	0.874	FRP Rupture	FRP Rupture
252	63	44	3	0.3	-14130.00	15	420	2000	3	1	1.52	19.847	19.193	0.967	FRP Rupture	FRP Rupture
253	15	22	3	0.3	-1766.25	30	420	500	0	0	1.00	1.227	1.000	0.815	Concrete Failure	Concrete Failure
254	15	22	3	0.3	-1766.25	30	420	500	1	0	1.41	13.641	13.110	0.961	FRP Rupture	FRP Rupture
255	15	22	3	0.3	-1766.25	30	420	500	2	1	1.64	26.054	25.547	0.981	FRP Rupture	Bar Rupture
256	15	22	3	0.3	-1766.25	30	420	500	3	1	1.63	27.000	23.225	0.860	Bar Rupture	Bar Rupture
257	33	30	3	0.3	-7065.00	30	420	1000	0	0	1.00	1.227	1.100	0.897	Concrete Failure	Concrete Failure
258	33	30	3	0.3	-7065.00	30	420	1000	1	0	1.24	7.434	7.401	0.996	FRP Rupture	FRP Rupture
259	33	30	3	0.3	-7065.00	30	420	1000	2	0	1.39	13.641	14.422	1.057	FRP Rupture	FRP Rupture
260	33	30	3	0.3	-7065.00	30	420	1000	3	1	1.52	19.847	21.113	1.064	FRP Rupture	FRP Rupture
261	63	44	3	0.3	-28260.00	30	420	2000	0	0	1.00	1.227	1.100	0.896	Concrete Failure	Concrete Failure
262	63	44	3	0.3	-28260.00	30	420	2000	1	0	1.13	4.330	3.797	0.877	FRP Rupture	FRP Rupture
263	63	44	3	0.3	-28260.00	30	420	2000	2	0	1.23	7.434	7.400	0.995	FRP Rupture	FRP Rupture
264	63	44	3	0.3	-28260.00	30	420	2000	3	0	1.31	10.537	10.834	1.028	FRP Rupture	FRP Rupture

No	n	$D_b$	$\rho$ %	$\frac{N}{f_c' A_g}$	N	$f_c'$	$f_y$	D	$t_j$	$\Phi$	$M_t / M_0$	DF wrt Parametric Equation (A)	DF From Computer Analysis (B)	B / A	Failure Mode with respect to Parametric Equation	Failure Mode with respect to Computer Analysis
265	15	22	3	0.4	-1177.50	15	420	500	0	0	1.00	1.026	1.000	0.975	Concrete Failure	Concrete Failure
266	15	22	3	0.4	-1177.50	15	420	500	1	1	1.89	20.236	19.194	0.949	FRP Rupture	FRP Rupture
267	15	22	3	0.4	-1177.50	15	420	500	2	2	2.06	27.000	23.226	0.860	Bar Rupture	Bar Rupture
268	15	22	3	0.4	-1177.50	15	420	500	3	2	2.04	27.000	21.113	0.782	Bar Rupture	Bar Rupture
269	33	30	3	0.4	-4710.00	15	420	1000	0	0	1.00	1.026	1.000	0.975	Concrete Failure	Concrete Failure
270	33	30	3	0.4	-4710.00	15	420	1000	1	0	1.55	10.631	9.850	0.927	FRP Rupture	FRP Rupture
271	33	30	3	0.4	-4710.00	15	420	1000	2	1	1.77	20.236	21.113	1.043	FRP Rupture	FRP Rupture
272	33	30	3	0.4	-4710.00	15	420	1000	3	1	1.96	27.000	28.102	1.041	Bar Rupture	Bar Rupture
273	63	44	3	0.4	-18840.00	15	420	2000	0	0	1.00	1.026	1.000	0.975	Concrete Failure	Concrete Failure
274	63	44	3	0.4	-18840.00	15	420	2000	1	0	1.36	5.828	5.559	0.954	FRP Rupture	FRP Rupture
275	63	44	3	0.4	-18840.00	15	420	2000	2	0	1.51	10.631	10.834	1.019	FRP Rupture	FRP Rupture
276	63	44	3	0.4	-18840.00	15	420	2000	3	1	1.63	15.433	15.866	1.028	FRP Rupture	FRP Rupture
277	15	22	3	0.4	-2355.00	30	420	500	0	0	1.00	1.026	1.000	0.975	Concrete Failure	Concrete Failure
278	15	22	3	0.4	-2355.00	30	420	500	1	0	1.54	10.631	10.835	1.019	FRP Rupture	FRP Rupture
279	15	22	3	0.4	-2355.00	30	420	500	2	1	1.81	20.236	21.114	1.043	FRP Rupture	FRP Rupture
280	15	22	3	0.4	-2355.00	30	420	500	3	1	1.88	27.000	23.226	0.860	Bar Rupture	Bar Rupture
281	33	30	3	0.4	-9420.00	30	420	1000	0	0	1.00	1.026	1.000	0.975	Concrete Failure	Concrete Failure
282	33	30	3	0.4	-9420.00	30	420	1000	1	0	1.34	5.828	6.116	1.049	FRP Rupture	FRP Rupture
283	33	30	3	0.4	-9420.00	30	420	1000	2	0	1.51	10.631	11.918	1.121	FRP Rupture	FRP Rupture

No	n	$D_b$	$\rho$ %	$\frac{N}{f_c' A_g}$	N	$f_c'$	$f_y$	D	$t_j$	$\Phi$	$M_t / M_0$	DF wrt Parametric Equation (A)	DF From Computer Analysis (B)	B / A	Failure Mode with respect to Parametric Equation	Failure Mode with respect to Computer Analysis
284	33	30	3	0.4	-9420.00	30	420	1000	3	1	1.64	15.433	17.449	1.131	FRP Rupture	FRP Rupture
285	63	44	3	0.4	-37680.00	30	420	2000	0	0	1.00	1.026	1.000	0.975	Concrete Failure	Concrete Failure
286	63	44	3	0.4	-37680.00	30	420	2000	1	0	1.20	3.427	3.139	0.916	FRP Rupture	FRP Rupture
287	63	44	3	0.4	-37680.00	30	420	2000	2	0	1.32	5.828	6.117	1.049	FRP Rupture	FRP Rupture
288	63	44	3	0.4	-37680.00	30	420	2000	3	0	1.41	8.230	8.956	1.088	FRP Rupture	FRP Rupture
289	15	26	4	0.1	-294.38	15	420	500	0	0	1.00	1.572	1.464	0.931	Concrete Failure	Concrete Failure
290	15	26	4	0.1	-294.38	15	420	500	1	1	1.53	27.000	25.548	0.946	Bar Rupture	FRP Rupture
291	15	26	4	0.1	-294.38	15	420	500	2	2	1.66	27.000	30.912	1.145	Bar Rupture	Bar Rupture
292	15	26	4	0.1	-294.38	15	420	500	3	2	1.67	27.000	30.912	1.145	Bar Rupture	Bar Rupture
293	35	34	4	0.1	-1177.50	15	420	1000	0	0	1.00	1.572	1.464	0.931	Concrete Failure	Concrete Failure
294	35	34	4	0.1	-1177.50	15	420	1000	1	0	1.32	16.174	14.421	0.892	FRP Rupture	FRP Rupture
295	35	34	4	0.1	-1177.50	15	420	1000	2	1	1.51	27.000	28.102	1.041	Bar Rupture	FRP Rupture
296	35	34	4	0.1	-1177.50	15	420	1000	3	1	1.59	27.000	28.102	1.041	Bar Rupture	Bar Rupture
297	50	56	4	0.1	-4710.00	15	420	2000	0	0	1.00	1.572	1.610	1.024	Concrete Failure	Concrete Failure
298	50	56	4	0.1	-4710.00	15	420	2000	1	0	1.19	8.873	8.955	1.009	FRP Rupture	FRP Rupture
299	50	56	4	0.1	-4710.00	15	420	2000	2	0	1.30	16.174	15.861	0.981	FRP Rupture	FRP Rupture
300	50	56	4	0.1	-4710.00	15	420	2000	3	1	1.41	23.474	25.545	1.088	FRP Rupture	FRP Rupture
301	15	26	4	0.1	-588.75	30	420	500	0	0	1.00	1.572	1.610	1.024	Concrete Failure	Concrete Failure
302	15	26	4	0.1	-588.75	30	420	500	1	0	1.33	16.174	19.194	1.187	FRP Rupture	FRP Rupture

No	n	$D_b$	$\rho$ %	$\frac{N}{f_c' A_g}$	N	$f_c'$	$f_y$	D	$t_j$	$\Phi$	$M_t / M_0$	DF wrt Parametric Equation (A)	DF From Computer Analysis (B)	B / A	Failure Mode with respect to Parametric Equation	Failure Mode with respect to Computer Analysis
303	15	26	4	0.1	-588.75	30	420	500	2	1	1.52	27.000	30.912	1.145	Bar Rupture	Bar Rupture
304	15	26	4	0.1	-588.75	30	420	500	3	1	1.52	27.000	30.912	1.145	Bar Rupture	Bar Rupture
305	35	34	4	0.1	-2355.00	30	420	1000	0	0	1.00	1.572	1.772	1.127	Concrete Failure	Concrete Failure
306	35	34	4	0.1	-2355.00	30	420	1000	1	0	1.18	8.873	10.835	1.221	FRP Rupture	FRP Rupture
307	35	34	4	0.1	-2355.00	30	420	1000	2	0	1.32	16.174	23.226	1.436	FRP Rupture	FRP Rupture
308	35	34	4	0.1	-2355.00	30	420	1000	3	1	1.44	23.474	30.913	1.317	FRP Rupture	Bar Rupture
309	50	56	4	0.1	-9420.00	30	420	2000	0	0	1.00	1.572	1.949	1.240	Concrete Failure	Concrete Failure
310	50	56	4	0.1	-9420.00	30	420	2000	1	0	1.09	5.222	6.728	1.288	FRP Rupture	FRP Rupture
311	50	56	4	0.1	-9420.00	30	420	2000	2	0	1.17	8.873	11.919	1.343	FRP Rupture	FRP Rupture
312	50	56	4	0.1	-9420.00	30	420	2000	3	0	1.25	12.523	17.451	1.393	FRP Rupture	FRP Rupture
313	15	26	4	0.2	-588.75	15	420	500	0	0	1.00	1.404	1.210	0.862	Concrete Failure	Concrete Failure
314	15	26	4	0.2	-588.75	15	420	500	1	1	1.57	27.000	23.225	0.860	Bar Rupture	FRP Rupture
315	15	26	4	0.2	-588.75	15	420	500	2	2	1.71	27.000	28.102	1.041	Bar Rupture	Bar Rupture
316	15	26	4	0.2	-588.75	15	420	500	3	2	1.73	27.000	28.102	1.041	Bar Rupture	Bar Rupture
317	35	34	4	0.2	-2355.00	15	420	1000	0	0	1.00	1.404	1.331	0.948	Concrete Failure	Concrete Failure
318	35	34	4	0.2	-2355.00	15	420	1000	1	0	1.35	14.287	13.110	0.918	FRP Rupture	FRP Rupture
319	35	34	4	0.2	-2355.00	15	420	1000	2	1	1.56	27.000	28.105	1.041	Bar Rupture	FRP Rupture
320	35	34	4	0.2	-2355.00	15	420	1000	3	1	1.65	27.000	30.916	1.145	Bar Rupture	FRP Rupture
321	50	56	4	0.2	-9420.00	15	420	2000	0	0	1.00	1.404	1.331	0.948	Concrete Failure	Concrete Failure

No	n	$D_b$	$\rho$ %	$\frac{N}{f_c' A_g}$	N	$f_c'$	$f_y$	D	$t_j$	$\Phi$	$M_t / M_0$	DF wrt Parametric Equation (A)	DF From Computer Analysis (B)	B / A	Failure Mode with respect to Parametric Equation	Failure Mode with respect to Computer Analysis
322	50	56	4	0.2	-9420.00	15	420	2000	1	0	1.22	7.846	7.399	0.943	FRP Rupture	FRP Rupture
323	50	56	4	0.2	-9420.00	15	420	2000	2	0	1.33	14.287	14.419	1.009	FRP Rupture	FRP Rupture
324	50	56	4	0.2	-9420.00	15	420	2000	3	1	1.45	20.729	23.223	1.120	FRP Rupture	FRP Rupture
325	15	26	4	0.2	-1177.50	30	420	500	0	0	1.00	1.404	1.331	0.948	Concrete Failure	Concrete Failure
326	15	26	4	0.2	-1177.50	30	420	500	1	0	1.34	14.287	15.863	1.110	FRP Rupture	FRP Rupture
327	15	26	4	0.2	-1177.50	30	420	500	2	1	1.57	27.000	28.102	1.041	Bar Rupture	FRP Rupture
328	15	26	4	0.2	-1177.50	30	420	500	3	1	1.61	27.000	28.102	1.041	Bar Rupture	Bar Rupture
329	35	34	4	0.2	-4710.00	30	420	1000	0	0	1.00	1.404	1.464	1.043	Concrete Failure	Concrete Failure
330	35	34	4	0.2	-4710.00	30	420	1000	1	0	1.20	7.846	8.954	1.141	FRP Rupture	FRP Rupture
331	35	34	4	0.2	-4710.00	30	420	1000	2	0	1.34	14.287	17.449	1.221	FRP Rupture	FRP Rupture
332	35	34	4	0.2	-4710.00	30	420	1000	3	1	1.45	20.729	23.227	1.121	FRP Rupture	FRP Rupture
333	50	56	4	0.2	-18840.00	30	420	2000	0	0	1.00	1.404	1.464	1.043	Concrete Failure	Concrete Failure
334	50	56	4	0.2	-18840.00	30	420	2000	1	0	1.10	4.625	5.054	1.093	FRP Rupture	FRP Rupture
335	50	56	4	0.2	-18840.00	30	420	2000	2	0	1.19	7.846	8.953	1.141	FRP Rupture	FRP Rupture
336	50	56	4	0.2	-18840.00	30	420	2000	3	0	1.26	11.066	13.109	1.185	FRP Rupture	FRP Rupture
337	15	26	4	0.3	-883.13	15	420	500	0	0	1.00	1.236	1.100	0.890	Concrete Failure	Concrete Failure
338	15	26	4	0.3	-883.13	15	420	500	1	1	1.64	23.566	21.113	0.896	FRP Rupture	FRP Rupture
339	15	26	4	0.3	-883.13	15	420	500	2	2	1.81	27.000	28.102	1.041	Bar Rupture	Bar Rupture
340	15	26	4	0.3	-883.13	15	420	500	3	2	1.82	27.000	25.548	0.946	Bar Rupture	Bar Rupture

No	n	$D_b$	$\rho$ %	$\frac{N}{f_c' A_g}$	N	$f_c'$	$f_y$	D	$t_j$	$\Phi$	$M_t / M_0$	DF wrt Parametric Equation (A)	DF From Computer Analysis (B)	B / A	Failure Mode with respect to Parametric Equation	Failure Mode with respect to Computer Analysis
341	35	34	4	0.3	-3532.50	15	420	1000	0	0	1.00	1.236	1.100	0.890	Concrete Failure	Concrete Failure
342	35	34	4	0.3	-3532.50	15	420	1000	1	0	1.40	12.401	11.919	0.961	FRP Rupture	FRP Rupture
343	35	34	4	0.3	-3532.50	15	420	1000	2	1	1.60	23.566	21.113	0.896	FRP Rupture	FRP Rupture
344	35	34	4	0.3	-3532.50	15	420	1000	3	1	1.75	27.000	30.912	1.145	Bar Rupture	Bar Rupture
345	50	56	4	0.3	-14130.00	15	420	2000	0	0	1.00	1.236	1.100	0.890	Concrete Failure	Concrete Failure
346	50	56	4	0.3	-14130.00	15	420	2000	1	0	1.26	6.818	6.116	0.897	FRP Rupture	FRP Rupture
347	50	56	4	0.3	-14130.00	15	420	2000	2	0	1.38	12.401	11.918	0.961	FRP Rupture	FRP Rupture
348	50	56	4	0.3	-14130.00	15	420	2000	3	1	1.49	17.983	17.448	0.970	FRP Rupture	FRP Rupture
349	15	26	4	0.3	-1766.25	30	420	500	0	0	1.00	1.236	1.000	0.809	Concrete Failure	Concrete Failure
350	15	26	4	0.3	-1766.25	30	420	500	1	0	1.41	12.401	13.110	1.057	FRP Rupture	FRP Rupture
351	15	26	4	0.3	-1766.25	30	420	500	2	1	1.64	23.566	23.225	0.986	FRP Rupture	FRP Rupture
352	15	26	4	0.3	-1766.25	30	420	500	3	1	1.72	27.000	25.548	0.946	Bar Rupture	Bar Rupture
353	35	34	4	0.3	-7065.00	30	420	1000	0	0	1.00	1.236	1.100	0.890	Concrete Failure	Concrete Failure
354	35	34	4	0.3	-7065.00	30	420	1000	1	0	1.24	6.818	7.401	1.085	FRP Rupture	FRP Rupture
355	35	34	4	0.3	-7065.00	30	420	1000	2	0	1.39	12.401	14.422	1.163	FRP Rupture	FRP Rupture
356	35	34	4	0.3	-7065.00	30	420	1000	3	1	1.50	17.983	19.194	1.067	FRP Rupture	FRP Rupture
357	50	56	4	0.3	-28260.00	30	420	2000	0	0	1.00	1.236	1.210	0.979	Concrete Failure	Concrete Failure
358	50	56	4	0.3	-28260.00	30	420	2000	1	0	1.14	4.027	4.177	1.037	FRP Rupture	FRP Rupture
359	50	56	4	0.3	-28260.00	30	420	2000	2	0	1.12	6.818	9.849	1.444	FRP Rupture	FRP Rupture

No	n	$D_b$	$\rho$ %	$\frac{N}{f_c' A_g}$	N	$f_c'$	$f_y$	D	$t_j$	$\Phi$	$M_t / M_0$	DF wrt Parametric Equation (A)	DF From Computer Analysis (B)	B / A	Failure Mode with respect to Parametric Equation	Failure Mode with respect to Computer Analysis
360	50	56	4	0.3	-28260.00	30	420	2000	3	0	1.31	9.610	10.834	1.127	FRP Rupture	FRP Rupture
361	15	26	4	0.4	-1177.50	15	420	500	0	0	1.00	1.068	1.000	0.936	Concrete Failure	Concrete Failure
362	15	26	4	0.4	-1177.50	15	420	500	1	1	1.74	19.961	19.194	0.962	FRP Rupture	FRP Rupture
363	15	26	4	0.4	-1177.50	15	420	500	2	2	1.96	27.000	28.102	1.041	Bar Rupture	Bar Rupture
364	15	26	4	0.4	-1177.50	15	420	500	3	2	1.95	27.000	23.226	0.860	Bar Rupture	Bar Rupture
365	35	34	4	0.4	-4710.00	15	420	1000	0	0	1.00	1.068	1.000	0.936	Concrete Failure	Concrete Failure
366	35	34	4	0.4	-4710.00	15	420	1000	1	0	1.48	10.514	9.850	0.937	FRP Rupture	FRP Rupture
367	35	34	4	0.4	-4710.00	15	420	1000	2	1	1.69	19.961	19.194	0.962	FRP Rupture	FRP Rupture
368	35	34	4	0.4	-4710.00	15	420	1000	3	1	1.88	27.000	28.102	1.041	Bar Rupture	FRP Rupture
369	50	56	4	0.4	-18840.00	15	420	2000	0	0	1.00	1.068	1.000	0.936	Concrete Failure	Concrete Failure
370	50	56	4	0.4	-18840.00	15	420	2000	1	0	1.32	5.791	5.559	0.960	FRP Rupture	FRP Rupture
371	50	56	4	0.4	-18840.00	15	420	2000	2	0	1.46	10.514	10.834	1.030	FRP Rupture	FRP Rupture
372	50	56	4	0.4	-18840.00	15	420	2000	3	1	1.56	15.238	15.866	1.041	FRP Rupture	FRP Rupture
373	15	26	4	0.4	-2355.00	30	420	500	0	0	1.00	1.068	1.000	0.936	Concrete Failure	Concrete Failure
374	15	26	4	0.4	-2355.00	30	420	500	1	0	1.53	10.514	10.835	1.030	FRP Rupture	FRP Rupture
375	15	26	4	0.4	-2355.00	30	420	500	2	1	1.77	19.961	21.114	1.058	FRP Rupture	FRP Rupture
376	15	26	4	0.4	-2355.00	30	420	500	3	1	1.88	27.000	23.226	0.860	Bar Rupture	Bar Rupture
377	35	34	4	0.4	-9420.00	30	420	1000	0	0	1.00	1.068	1.000	0.936	Concrete Failure	Concrete Failure
378	35	34	4	0.4	-9420.00	30	420	1000	1	0	1.32	5.791	5.560	0.960	FRP Rupture	FRP Rupture

No	n	$D_b$	$\rho$ %	$\frac{N}{f_c' A_g}$	N	$f_c'$	$f_y$	D	$t_j$	$\Phi$	$M_t / M_0$	DF wrt Parametric Equation (A)	DF From Computer Analysis (B)	B / A	Failure Mode with respect to Parametric Equation	Failure Mode with respect to Computer Analysis
379	35	34	4	0.4	-9420.00	30	420	1000	2	0	1.49	10.514	11.918	1.133	FRP Rupture	FRP Rupture
380	35	34	4	0.4	-9420.00	30	420	1000	3	1	1.61	15.238	15.863	1.041	FRP Rupture	FRP Rupture
381	50	56	4	0.4	-37680.00	30	420	2000	0	0	1.00	1.068	1.000	0.936	Concrete Failure	Concrete Failure
382	50	56	4	0.4	-37680.00	30	420	2000	1	0	1.19	3.430	2.853	0.832	FRP Rupture	FRP Rupture
383	50	56	4	0.4	-37680.00	30	420	2000	2	0	1.30	5.791	6.117	1.056	FRP Rupture	FRP Rupture
384	50	56	4	0.4	-37680.00	30	420	2000	3	0	1.39	8.153	8.956	1.098	FRP Rupture	FRP Rupture